AD-A033 289 CALIFORNIA UNIV LOS ANGELES DEPT OF COMPUTER SCIENCE F/G 14/5
PICTURE DECOMPOSITION, TREE DATA-STRUCTURES AND IDENTIFYING DIR--ETC(U)
SEP 76 N ALEXANDRIDIS, A KLINGER AF-AFOSR-2384-72
UNCLASSIFIED UCLA-ENG-7684 AFOSR-TR-76-1220 NL

1 OF 2
AD A033289

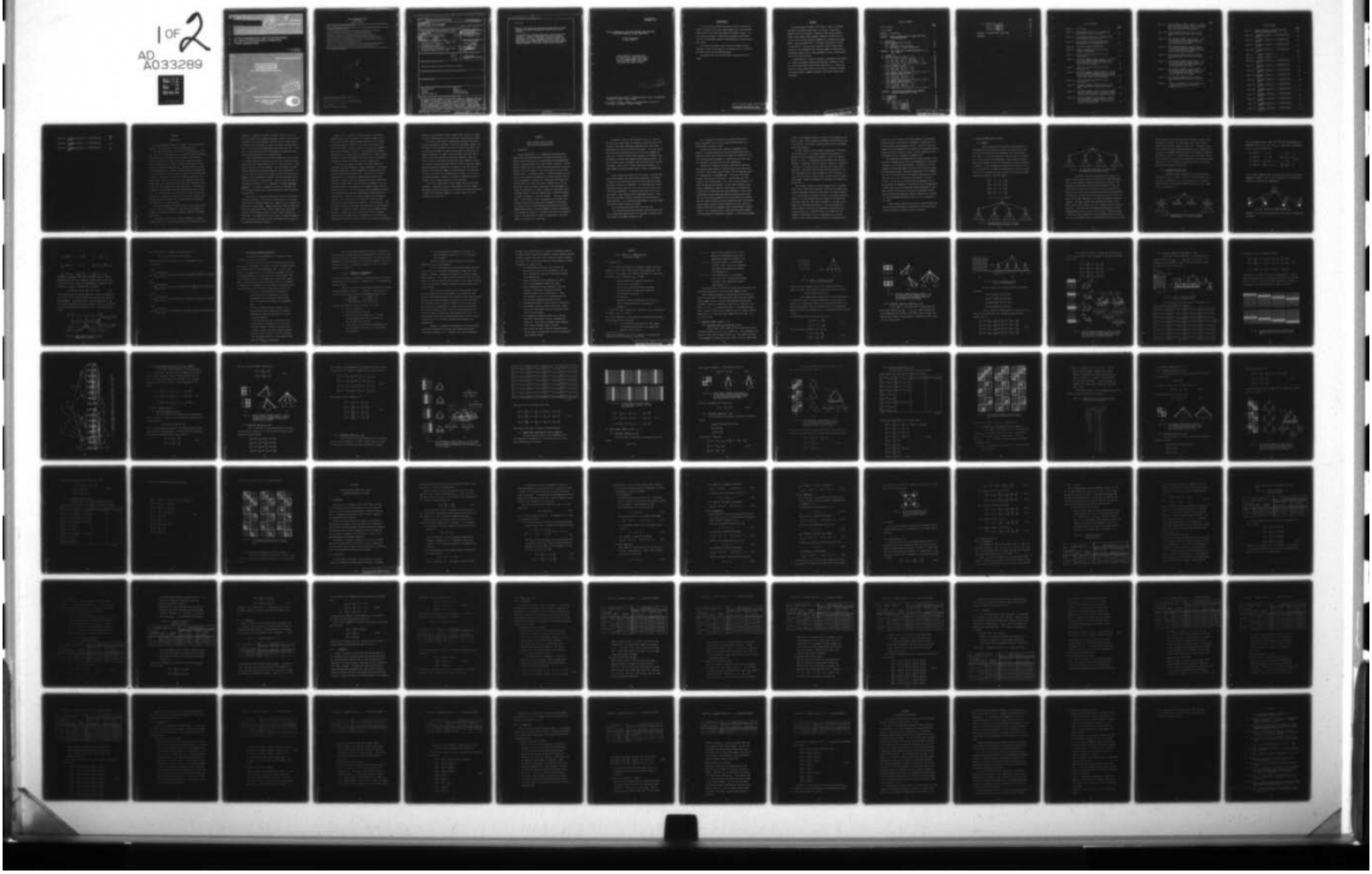


OF
3289

UCLA-ENG-7684

Date Published – SEPTEMBER 1976

PICTURE DECOMPOSITION, TREE DATA-STRUCTURES, AND IDENTIFYING DIRECTIONAL SYMMETRIES AS NODE COMBINATIONS

N. ALEXANDRIDIS
A. KLINGER

COMPUTER METHODOLOGY GROUP

Research partially supported by the
Air Force Office of Scientific Research
Air Force Systems Command, USAF
under Grant No. AFOSR-72-2384
titled "Statistical Models and Computer Systems."

COMPUTER SCIENCE DEPARTMENT

School of Engineering and Applied Science
University of California
Los Angeles

COMPUTER METHODOLOGY GROUP
REPORT SERIES

Allen Klinger, Series Editor

Automatic Computer Studies of the Atmospheric Diffusion of Air Pollutants in the Presence of Photochemical Reactions, W.J. Karplus, J. Keansley and L. Barnett, No. 59-2, January 1959.

A Measure of the Significance of Pattern Features for Use as an Aid in the Design of Recognition Systems (Digital Tech. Job No. 815), C. Maltz, No. 62-68, December 18, 1962.

The Hadamard Transform in Image Processing and Pattern Recognition, N.A. Alexandridis, No. 70-11, March 1970.

Application of Walsh Transform to Statistical Analysis, J. Pearl, UCLA-ENG-7072, August 1970.

Walsh-Hadamard Transformations in Image Processing, N.A. Alexandridis, UCLA-ENG-7108, March 1971.

The Application of the DSDT Hybrid Computer Method to Water Resources Problems, UCLA-ENG-7142, June 1971.

Distributed Parameter Systems (An Annotated Bibliography — to April 1971, L. Johnsson, UCLA-ENG-7143, August 1971.

Reliability in Computing Systems, A. Klinger, UCLA-ENG-7258, July 1972.

The Application of the Digital Simulation Language PDEL to Subsurface Hydrology Problems, UCLA-ENG-7432, April 1974.

Analysis and Design of Relational Schemata for Database Systems, C.A. Zaniolo, UCLA-ENG-7669, July 1976.

Picture Decomposition, Tree Data-Structures, and Identifying Directional Symmetries as Node Combinations, N. Alexandridis and A. Klinger, UCLA-ENG-7684, September 1976.

UNCLASSIFIED

SECURITY CLASSIFICATION OF THIS PAGE (When Data Entered)

REPORT DOCUMENTATION PAGE	READ INSTRUCTIONS BEFORE COMPLETING FORM
1. REPORT NUMBER: AFOSR-TR-76-1220	2. GOVT ACCESSION NO. / 3. RECIPIENT'S CATALOG NUMBER
4. TITLE (and Subtitle): PICTURE DECOMPOSITION, TREE DATA-STRUCTURES AND IDENTIFYING DIRECTIONAL SYMMETRIES AND NODE COMBINATIONS	5. TYPE OF REPORT & PERIOD COVERED: Interim rept.
	6. PERFORMING ORG. REPORT NUMBER: UCLA-ENG-7684
7. AUTHOR(s): I./Alexandridis A./Klinger (Nikitas Allen)	8. CONTRACT OR GRANT NUMBER(s): AF-AFOSR 72-2384-72
9. PERFORMING ORGANIZATION NAME AND ADDRESS: University of California, Computer Science Department, Los Angeles, CA 90024	10. PROGRAM ELEMENT, PROJECT, TASK AREA & WORK UNIT NUMBERS: 61102F 2304/A2
11. CONTROLLING OFFICE NAME AND ADDRESS: Air Force Office of Scientific Research/NM, Bolling AFB, Washington, DC 20332	12. REPORT DATE: September 1976
	13. NUMBER OF PAGES: 88
14. MONITORING AGENCY NAME & ADDRESS (if different from Controlling Office)	15. SECURITY CLASS. (of this report): UNCLASSIFIED
	15a. DECLASSIFICATION/DOWNGRADING SCHEDULE

16. DISTRIBUTION STATEMENT (of this Report)

Approved for public release; distribution unlimited.

17. DISTRIBUTION STATEMENT (of the abstract entered in Block 20, if different from Report)

18. SUPPLEMENTARY NOTES

19. KEY WORDS (Continue on reverse side if necessary and identify by block number)

data structures	search
feature	symmetries
indexing	syntactic methods
pattern recognition	tree representation

20. ABSTRACT (Continue on reverse side if necessary and identify by block number)

The general problem treated in this report is that of extracting structural information from an object in a scene. In particular, symmetries are used as another--in addition to the average intensity values--global coarse picture parameter subregion characteristic, of a picture that has been regularly decomposed to a dimensionally reduced subset. Regular decomposition is a procedure through which a picture is subdivided in a particular way, leading to a data structure representation of the information which preserves

DD FORM 1 JAN 73 1473 EDITION OF 1 NOV 65 IS OBSOLETE

UNCLASSIFIED

SECURITY CLASSIFICATION OF THIS PAGE (When Data Entered)

20 Abstract

geometric and topological relationships among pixels or among aggregates of pixels (substructures) found in the original picture.

A proposition for a recursive algorithm is given which, when applied to a regularly decomposed picture whose important information is kept in a tree data-structure, specifies the tree nodes (i.e., picture subregions of various sizes) that must be paired (or compared) to identify (or extract) possible symmetries present in the figure, along various directions.

UCLA-ENG-7684
SEPTEMBER, 1976

PICTURE DECOMPOSITION, TREE DATA-STRUCTURES, AND IDENTIFYING DIRECTIONAL SYMMETRIES AS NODE COMBINATIONS

Nikitas Alexandridis*
Allen Klinger**

Research partially supported by the Air Force Office of Scientific Research, Air Force Systems Command, USAF, under Grant No. AFOSR-72-2384 titled "Statistical Models and Computer Systems."

* N. Alexandridis has the Chair of Computer Science, School of Engineering, University of Patras, Patras, Greece.

** A. Klinger, Professor, Computer Science Department, University of California, Los Angeles, California 90024.

ACKNOWLEDGMENT

This research was partially sponsored by the Air Force Office of Scientific Research, Air Force Systems Command, USAF, under Grant No. AFOSR-72-2384 titled "Statistical Models and Computer Systems." The United States Government is authorized to reproduce and distribute reprints for Governmental purposes notwithstanding any copyright notation hereon.

This research was mainly carried out at the Computer Science Department of UCLA, while Professor N. Alexandridis was visiting UCLA and working under the above-mentioned grant.

The authors would like to express their appreciation for this support.

ABSTRACT

The general problem treated in this report is that of extracting structural information from an object in a scene. In particular, symmetries are used as another--in addition to the average intensity values--global coarse picture parameter subregion characteristic, of a picture that has been regularly decomposed to a dimensionally reduced subset. *Regular decomposition* is a procedure through which a picture is subdivided in a particular way, leading to a data structure representation of the information which preserves geometric and topological relationships among pixels or among aggregates of pixels (substructures) found in the original picture.

A proposition for a recursive algorithm is given which, when applied to a regularly decomposed picture whose important information is kept in a tree data-structure, specifies the tree nodes (i.e., picture subregions of various sizes) that must be paired (or compared) to identify (or extract) possible symmetries present in the figure, along various directions.

TABLE OF CONTENTS

LIST OF FIGURES

LIST OF TABLES

SECTION 1

INTRODUCTION

The general problem treated in this report is that of extracting structural information from a regularly decomposed picture.

The theme of this report is that the key to effective use of digital computers in picture processing is in partitioning before applying local techniques. A characteristic of the human picture analysis process is a hierarchical type of functioning. People first group data in perceptual levels; these are then further grouped into subdivisions. Experiments conducted [42] on the ways we describe aerial terrain photographs--or, in general, complex pictures--concluded that: (1) if a picture has a central theme, we respond to it and relate other portions to it and (2) if a picture has no central theme, but is totally diffuse, we partition the picture into quadrants ("upper right", "upper left", etc.) and either describe each region separately or the objects within the quadrants and their relationships. The analysis of a complex picture by computer can often be broken down into two steps [47]: (a) Discrimination of "uniform regions" within the picture (a region can be "uniform" with respect to values of any of several local properties) and (b) description of figures within the picture which can be built up out of these regions.

The regular decomposition scheme [2-3, 36-37] of the next section divides a picture into subquadrants. These are either further subdivided or discarded according to the amount of important information they contain.

The conjecture [18] that use of global information can improve computer analysis of pictures (compared with blind application of local

operators) is supported by results. The application of a local criterion too often destroys needed information. However, the main problem encountered in the global methods is the fact that the search space is very large, tens of thousands of points in a picture, and the combinatorics of the problem force unacceptably long search times [45]. Therefore, in the field of Artificial Intelligence much research has been done on developing heuristics for reducing search.

Regular decomposition is a hierarchical method for search of practical representations of scenes based on recursion via subblock storage. Average grey level intensity over the cells in a given subblock is used below as the decision-driving parameter. Our tree structure provides implicit topological relationships among the picture subquadrants. At a specific level of the tree, all existing entities (for brevity we use entity to mean any subquadrant retained in the tree representation of a picture) are uniform in size and shape. The tree levels give implicit relationships ("belongs to" or "is contained in") between nonuniform entities: i.e., groups of subquadrants, possibly of different size. This tree data structure can be searched and picture objects retrieved by processing it.

The analysis of a difficult problem often leads to the discovery of symmetries, and these in turn lead to a simplification of the problem. Simplification of problems through use of symmetries can be viewed as an application of group theory. Symmetry groups are a part of algebra but they also relate to the field of graphs. Specifically, they permit identification of whether a graph is invariant under rotations and reflections. Also symmetries are used in games, to reduce the number of distinct decisions to be made or moves to be taken, and in puzzles to help reduce the search for solutions.

Natural objects, as well as man-made structures and symbols, frequently possess axes of symmetry. An elementary example of pictorial objects divided by their symmetry properties are the letters of the Roman alphabet. Polya [1, p. 89, prob. 18] noted that subsets with horizontal, vertical, central, all three, and no symmetries exist within the twenty-six letters. Since classifying an unknown image pattern by a limited series of measurements is a typical pattern recognition problem, using symmetry data aids in that in the example of alphabetic characters and may do so in more general cases.

In order to use symmetry properties in computer processing of visual data (such as photographs or graphic displays), it is necessary to develop algorithms to evaluate symmetries in two-dimensional data sets with minimum computational effort. This report is an initial investigation of the theoretical properties which underlie such algorithms. The calculations are applied to the area of pattern perception by automatic means. We are primarily concerned with carrying the regular decomposition procedure into structural feature identification and extraction. We first apply the regular decomposition scheme to a picture and then work with a dimensionally-reduced data base: a structured tree. Our goal in extracting symmetry data from general pictures is to aid registration ("lining up" or locating of key directions), object location, and recognition. We are trying to: identify existing relationships between tree nodes and structural features of objects. In general, structural features include symmetry, shape, perimeter, straight lines, etc. We also wish to derive (optimum) algorithms for extracting structural information from the tree representation of an object and for identifying invariant picture substructures.

Finally, we seek to define "uniform" regions, where uniformity is based not only on intensity but also on the structural properties of an object.

The results are set forth as propositions regarding levels within a grid superimposed on a picture. By recursive refinement (deeper levels are found in finer partitions of the picture region) these propositions can be applied to reduce the computing time needed to characterize the symmetry properties of a scene. Results obtained include the identification of tree nodes that must be paired (or compared) at each tree level in order to identify (and extract) directional symmetries present in a picture. When searching the tree for a certain directional symmetry, we stop examining the successors to a node pair if that pair does not belong to the directional symmetry set being examined. We incorporate "no move to next level if the examined pair of nodes is not a class of the examined symmetry" (successors can never be combined to yield this symmetry class at higher resolution) in our algorithms.

The initial investigation we report regards only four directional symmetries: horizontal, vertical, right diagonal, and left diagonal. We propose a recursive algorithm for identifying tree nodes corresponding to these four directional symmetries at various degrees of picture resolutions (or tree levels).

SECTION 2

REGULAR DECOMPOSITION OF PICTURES (AND THEIR TREE-REPRESENTATIONS)

2.1 INTRODUCTION

"Picture digitization", i.e., converting the two-dimensional analog signal into digital, preceeds any application of digital computers to picture processing. Digitized pictures are two-dimensional arrays of "picture elements" (or pixels) similar to matrices. Electro-optical scanners are used to perform this analog-to-digital conversion, and each pixel is an average of local light intensity in the picture around a point. This average intensity is usually quantized, for real pictures in an eight-level quantization, and thus the digital form of a pixel corresponds to an 8-bit byte. Through the most oftenly used "raster-scanner" or "flying spot scanner" (although as we will see below, other types of picture scanning may be more advantageous), a picture is represented as a series of bytes which correspond to first row leftmost point...first row rightmost point...second row leftmost ...second row rightmost ... last row leftmost ... last row rightmost point. In this "series of rows" representation, the "points" have a nonzero diameter given by the optical properties of the scanner. The "spread" or spot size and averaging characteristics may differ between scanning devices, as may the number of levels of quantization of the average value stored. In addition, pixels will not correspond exactly to the same points or spots in a picture even if the same scanner is used twice on a given image.

In quantity, a 500 row, 500 points per row array, or briefly a 500 x 500 array, would roughly correspond to a television image, while pictures of real scenes (military reconnaisance data, radar multi-target data, etc.) are of size 1024 x 1024 points. It is seen, therefore, that we are talking on the order of 10^6 picture elements (or bytes), and in trying to handle them by computers we immediately face the storage limitations that computer central memories present. The same limitations occur in processing time series data such as electrocardiograms - where events of similar shape occur repeatedly - or other biomedical applications data, such as x-rays, chromosome cells, etc.

A major common characteristic of such pictures is the fact that not all these sampled data convey useful information. For example, in scenes of aerial photographs large areas of the photo are uniform, thus being of little or no importance. In time series data, certain "regularities" and "repetitions" exist which add very little to the total useful information. In processing these data, little or no time should be spent looking at those noninformative areas. Therefore, the key problem to pattern recognition and scene analysis is "data reduction", i.e., filtering out noninformative areas and keeping only the more complex portion of the data.

Two of the many ways by which this can be done are:

(1) by structuring the data according to goal-oriented criteria (e.g., through data reduction heuristics designed to eliminate particular kinds of irrelevant information), and

(2) by subdividing the problem into smaller and easier-to-handle subproblems (e.g., by restricting the problem domain to a limited number of possible inputs).

The above two ways are not necessarily independent of one another. All problem solving activities are characterized by these properties of data "over-richness" and problem "over-complexity", the first requiring search procedures for identifying useful data structure formations, the second involving task segmentation.

Separation of "objects" from their noninformative background has long been a major concern in pattern recognition and scene analysis [8-10]. Many isolated objects present in a two-dimensional array is a characteristic of chromosome data. In [11] over 10^6 scanned elements, from more than forty objects in one picture, were first reduced to some 10^4 data points, each a left or right end point of an object at some vertical ordinate. A similar data structure is presented in [12] where a system for picture search is presented which is applicable to contour maps and aerial photographs. Direct object identification was also done algorithmically, employing edge detection and line fitting procedures [13-15] while others have performed extensive analysis relating to region properties (union, intersection, common boundary) [16-19], distance properties [12, 21], chaining of boundary points [22] and subsequent direct identification of separate objects. In an analogous fashion, Barrow and Milner [25] suggested a similar approach for hierarchical synthesis. In [26], they performed

a match in an incremental fashion by building up correspondences, one pair at a time. A partial match was evaluated by determining how many of the relations in the model structure agreed with their corresponding picture relations.

All these techniques have the major disadvantage of investigating long tape files (i.e., exhaustive point-by-point search) to determine structural properties of groups of pixels or to identify objects in a scene - a cumbersome and large-computer-time consuming procedure. Furthermore, since they involve a "bottom-up" segmentation - the use of raster point values to build up a more global picture description - they require local picture processing operations first to be performed, with all their related local noise influences [16]. Thus, the trivial cases of large uniform-intensity regions (noninformative areas), consume an unnecessarily large amount of computer processing time.

The "top-down" approach of regular decompositions of two-dimensional arrays (subdividing the problem into smaller and simpler ones) has been independently proposed by many workers in computer graphics [23], scene analysis, architectural design [6] and pattern recognition. Warnock [4, 20] used successively finer squares in his hidden-line-elimination algorithm. SRI's mobile automaton [5] utilizes a "grid-model" which subdivides the automaton's visual environment to an arbitrary degree of precision for determining the feasibility of a proposed journey path. Many others have also followed this "decomposition-into-regions" idea as a preprocessing step to their analysis. Barrow and Popplestone [24] were first converting the TV

picture into a set of regions of uniform brightness and were determining properties of those regions (compactness, triangularity) and relations between them (adjacency, left of). Then this structure of regions with given properties and relations was in turn matched against standard structures previously stored. A similar procedure of regular decomposition was independently proposed in [2].

The advantage of the decomposition or top-down approach is that the previous extremely local raster scan representation is now being replaced by a more global data-structure. Furthermore, this way of processing pictorial data spends little or no time looking at simple and noninformative areas. Two major disadvantages of this decomposition are: (1) the arbitariness of the regular decomposition dividing lines for areas and (2) the decision rule whether to "partition farther". The two ways of overcoming these disadvantages, that of using neighboring subquadrants to "soften" the regular decomposition boundary lines, and that of performing adaptive adjustment of parameter threshold values will be discussed in a subsequent section. Ways of incorporating additional subregion characteristics, besides just average subregion intensity values, will also be suggested in this report.

In the following section we describe the regular-decomposition image-processing algorithm for structuring the picture data and obtaining informative or complex portions of a picture.

2.2 REGULAR DECOMPOSITION OF PICTURES

2.2.1 General

There are many ways of performing the two-dimensional to one-dimensional transformation of pictures, the raster scan or line-by-line digitization and serial storage being the simpler and most often used. It is also well known that a picture array can be thought of as a special case of a tree-structure. The particular equivalent tree-structure depends on the pixel relationships we want to exemplify. For example, Fig. 2.2 represents the equivalent tree-structure of the 4 x 4 picture of Fig. 2.1 where row relationships are explicitly shown, while Fig. 2.3 represents the tree-structure of the same picture where column relationships are explicitly shown.

$$\begin{bmatrix} P_{11} & P_{12} & P_{13} & P_{14} \\ P_{21} & P_{22} & P_{23} & P_{24} \\ P_{31} & P_{32} & P_{33} & P_{34} \\ P_{41} & P_{42} & P_{43} & P_{44} \end{bmatrix}$$

Fig. 2.1: A 4 x 4 Picture

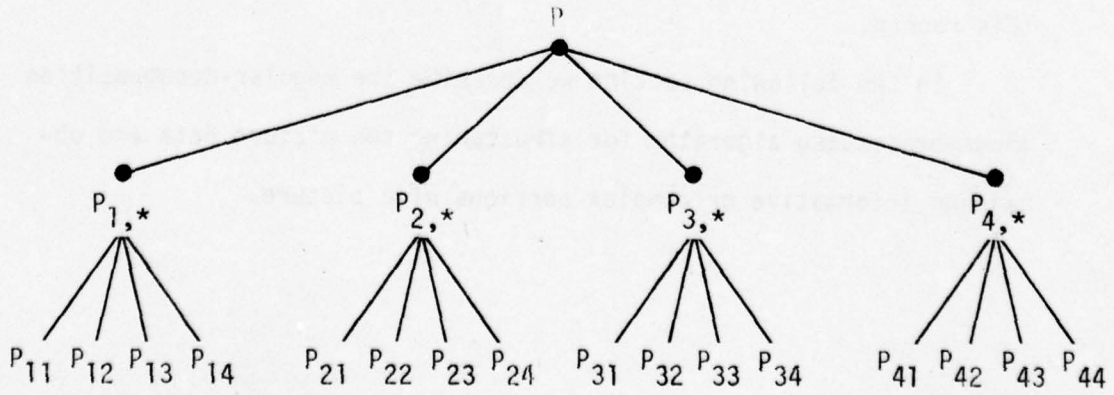

Fig. 2.2: The Equivalent Tree of Fig. 2.1, Where Row Relationships Are Explicitly Shown.

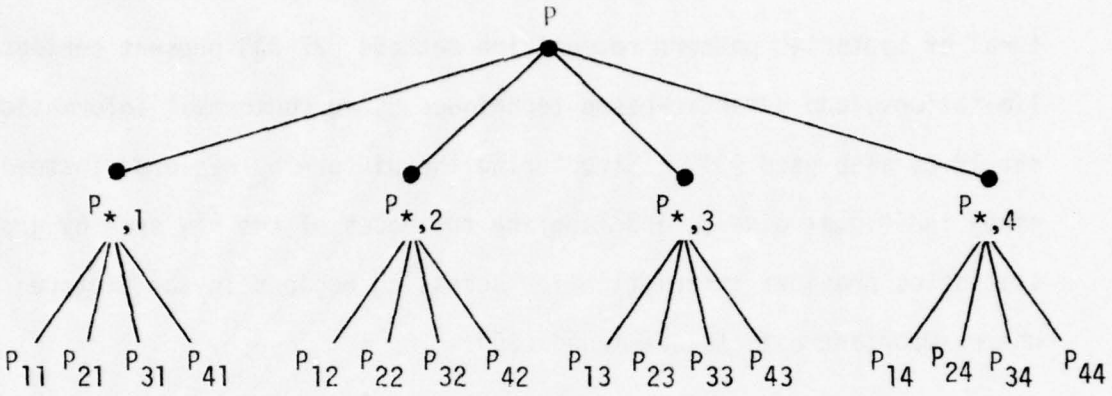

Fig. 2.3: The Equivalent Tree of Fig. 2.1, Where Column Relationships are Explicitly Shown.

In neither of the two tree representations however, i.e., neither in the series-of-rows nor in the series-of-columns representations, are the geometric relationships among pixels preserved. The particular way one chooses to build the data structure reflects the user's priorities about the accessibility of certain properties contained within the data base, and the above-mentioned two representations yield the least desirable way of storing and accessing the picture elements and the most cumbersome way of identifying geometric features of objects in the image. Besides these horizontal and vertical lines, there are many other straight lines (e.g., diagonal lines) or line segments (e.g., lines that result from applying edge operators like the pseudogradient) that we can define for the picture. Important aspects in the scene analysis procedure are line interrelationships, line densities, etc. Furthermore, only local intensity has been used as the coarse

picture parameter, while other more global parameters, features (which are aggregates of pixels) and relationships may be better (such as average region intensity, symmetry, shape, etc.). Furthermore, structural or syntactic pattern recognition methods [27-33] present serious limitations, and semantic-based techniques using contextual information should be also used [34]. Structuring the picture by regions, instead of by individual pixels, and labeling the nodes of the new tree by gross statistics provides information for accessing regions in the picture where important objects are found [35].

2.2.2 Subquadrant Tree Structures

Through the regular decomposition, the equivalent tree-structure of Fig. 2.1 is given in Fig. 2.4. The entire picture array P has four subquadrants P_a, P_b, P_c, and P_d and this tree structure directly reflects area coherence rather than row (Fig. 2.2) or column (Fig. 2.3) coherence [37].

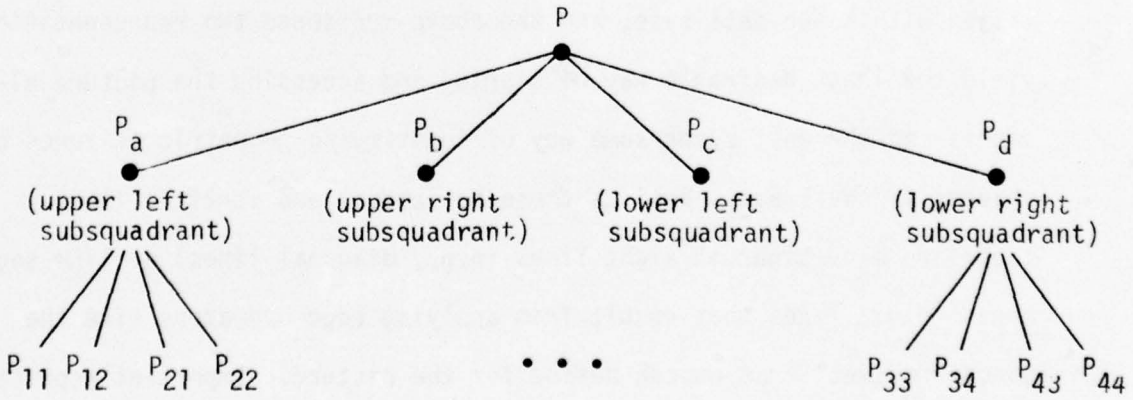

Fig. 2.4: Tree-structure Resulting From the Regular Decomposition of a 4 x 4 Picture Array P.

For an nxn square picture P, where its i^{th} row j^{th} column elements are denoted by P[i,j], i=1,2,...,n, j=1,2,...,n, then the four subquadrants P_a, P_b, P_c, P_d are given by [37]:

$$\begin{aligned}
P_a &= \left\{P[i,j] : \quad 1 \le i \le \frac{n}{2} \quad , \quad 1 \le j \le \frac{n}{2} \right\} \\
P_b &= \left\{P[i,j] : \quad 1 \le i \le \frac{n}{2} \quad , \quad \left(\frac{n}{2}+1\right) \le j \le n \right\} \\
P_c &= \left\{P[i,j] : \quad \left(\frac{n}{2}+1\right) \le i \le n \quad , \quad 1 \le j \le \frac{n}{2} \right\} \\
P_d &= \left\{P[i,j] : \quad \left(\frac{n}{2}+1\right) \le i \le n \quad , \quad \left(\frac{n}{2}+1\right) \le j \le n \right\}
\end{aligned} \tag{2.1}$$

In [37] a useful method is given for locating the center of such regular decomposition regions. Fig. 2.5 below illustrates this quadrantization scheme for a single level of decomposition.

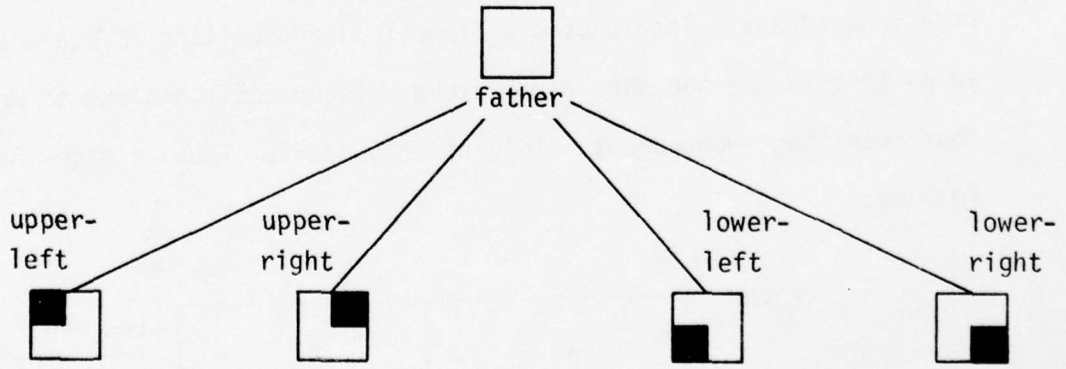

Fig. 2.5: One Level of Regular Decomposition.

Equations 2.1 can be easily carried out to a second level of decomposition as follows:

$$P_{aa} = \left\{ P[i,j] \;:\; 1 \le i \le \frac{n}{4} \;,\; 1 \le j \le \frac{n}{4} \right\}$$

$$\vdots$$

$$P_{ba} = \left\{ P[i,j] \;:\; 1 \le i \le \frac{n}{4} \;,\; \left(\frac{n}{2} + 1\right) \le j \le \frac{3n}{4} \right\} \quad (2.2)$$

$$\vdots$$

$$P_{dd} = \left\{ P[i,j] \;:\; \left(\frac{3n}{4} + 1\right) \le i \le n \;,\; \left(\frac{3n}{4} + 1\right) \le j \le n \right\}$$

Informally, a quadrant is a discrete, rectangular area of a picture characterized in terms of its intensity, relative position within the picture, and its size. Hence, for implementation, a quadrant is characterized by a 5-tuple of characteristics as follows:

$$C = \langle \text{Intensity, x\_min, x\_max, y\_min, y\_max} \rangle \quad (2.3)$$

For the general case, the quadrant subdivision is done by dividing each of its sides in half and then assigning the appropriate new vertices to each subquadrant. The functions floor ($\lfloor\ \rfloor$) and ceiling ($\lceil\ \rceil$) are used so as to make the boundary lines along integer positions and to make the four resulting subquadrants disjoint (Fig. 2.6). These are defined as follows:

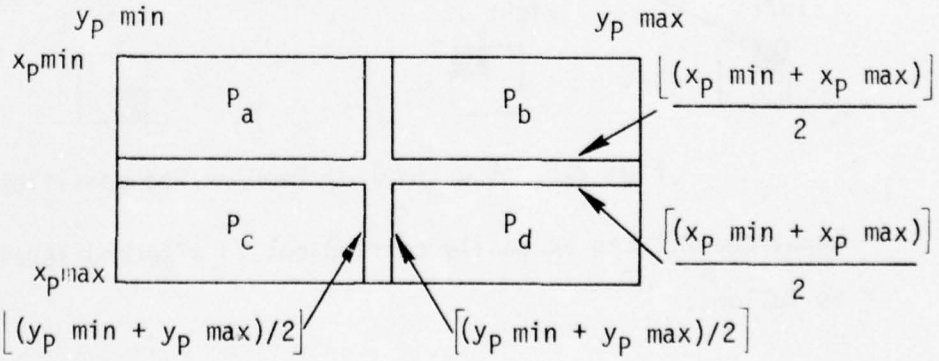

Fig. 2.6: Integer Boundary Values of the Four Subquadrants of Quadrant P.

Let P be the label of a quadrant whose properties are C_P :

$$C_P = \langle I_P,\ x_P\ \min,\ x_P\ \max,\ y_P\ \min,\ y_P\ \max \rangle$$

Then the root-labels and properties of its four subquadrants P_a, P_b, P_c and P_d are:

1) P_a

$$C_{Pa} = \langle \int_{y_{Pa}min}^{y_{Pa}max} \int_{x_{Pa}min}^{x_{Pa}max} I(x,y)dxdy, x_P min, \left\lfloor (x_P min + x_P max)/2 \right\rfloor, y_P min, \left\lfloor (y_P min + y_P max)/2 \right\rfloor \rangle$$

2) P_b

$$C_{Pb} = \langle \int_{y_{Pb}min}^{y_{Pb}max} \int_{x_{Pb}min}^{x_{Pb}max} I(x,y)dxdy, x_P min, \left\lfloor (x_P min + x_P max)/2 \right\rfloor, \left\lceil (y_P min + y_P max)/2 \right\rceil, y_P max \rangle$$

3) P_c

$$C_{Pc} = \langle \int_{y_{Pc}min}^{y_{Pc}max} \int_{x_{Pc}min}^{x_{Pc}max} I(x,y)dxdy, \left\lceil (x_P min + x_P max)/2 \right\rceil, x_P max, y_P min, \left\lfloor (y_P min + y_P max)/2 \right\rfloor \rangle$$

4) P_d

$$C_{Pd} = \langle \int_{y_{Pd}min}^{y_{Pd}max} \int_{x_{Pd}min}^{x_{Pd}max} I(x,y)dxdy, \left\lceil (x_P min + x_P max)/2 \right\rceil, x_P max, \left\lceil (y_P min + y_P max)/2 \right\rceil, y_P max \rangle$$

2.2.3 Methodology of Regular Decomposition

The way this picture decomposition in quadrants is being performed is as follows [2-3, 36-37]:

Initially, the entire picture two-dimensional array of gray level values is considered as a quadrant. We examine the whole quadrant to see whether there is anything informative there. The two critical issues in this procedure are: (1) to define an "importance factor" for the area examined which will give a measure of "informativeness" (this is very difficult because, in the general case, both syntactic and semantic information must be taken into account), and (2) to incorporate an appropriate discrimination function for looking into further details of the informative area. The following three possible cases exist:

1. If the area is characterized as noninformative, then that area of the picture may be eliminated from the data structure without significant data loss. Such cases are for example large homogeneous areas.
2. The area is characterized very informative (the discrimination function identifies many important features) and, therefore, this data must be saved in the data structure.
3. In the third case, the area is characterized with enough importance that makes us--at least so far--not sure on whether it should be eliminated from or whether it should be saved in the data structure. The picture must, therefore, be further subdivided into four quadrants and ask the same questions about each one of these four subquadrants.

So far we have been experimenting using only intensities as the coarse picture parameter and obtaining experimental results by thresholding the picture using various threshold values. The importance of any subquadrant is defined relative to only its parent quadrant. The relative importance $d(P,P_\star)$ of a subquadrant $P_\star$ (where $\star$ = a,b,c or d) within a quadrant P is defined as:

$$d(P,P_\star) = \frac{\text{Intensity of subquadrant } P_\star}{\text{Intensity of quadrant P}}$$

This, $d(P,P_\star)$ represents a percentage of information relative to the surrounding area, and this function is convenient since it is independent of depth in the tree.

The picture description function $\alpha(d) = \alpha(d(P,P_\star))$ is defined as the importance of a quadrant $P_\star$ in picture P. The following is an arbitrary discrimination function using threshold values Θ_1 and Θ_2 :

$$\alpha(d) = \begin{cases} \text{informative}, & \Theta_2 \le d(P,P_\star) \le 1.0 \\ \text{not sure}, & \Theta_1 \le d(P,P_\star) < \Theta_2 \\ \text{non-informative}, & 0.0 \le d(P,P_\star) < \Theta_1 \end{cases}$$

Thus, the data-structure-creating algorithm is as follows:

1. Find total intensity.
2. Partition into four subregions.
3. Refine any "not sure" subregion, i.e., one with intensity greater than Θ_1 and less than Θ_2 of the one higher level intensity.
4. Do not retain any "non-informative" subregion, i.e., one with intensity less than Θ_1 of the one higher level intensity.

5. Stop refining, when an "informative" subregion, i.e., one with intensity greater than Θ_2 of the one higher level intensity.

There are two ways of actually implementing the picture decomposition into its tree quadrants:

The first way corresponds to the bottom-up method, operating on long "tape-files" that have been generated by a common raster scan procedure. Therefore, adaptation and processing of the actual sampled image is necessary. This is done by bringing into main core a few "line slices" at a time and processing them to extract all the useful information for the tree generation. Quadrant subpictures represent compact areas of picture elements.

The second way corresponds to the top-down method, assumes that the sequential nature of tape records is an inappropriate data structure and therefore eliminates the conventional raster scan techniques. Unconventional scanning equipment could be built to retain information about neighboring pixels and picture quadrants and to evaluate local logical functions to decide which are likely structural relationships. Data could be obtained by logical circuitry clocking performing non-uniform and adaptive picture scans under computer control [38]. This second method leads directly to hardware (processing of parallel sensed picture points) [39] or software (parallel picture grammars) [40] implementations.

Details of overcoming the disadvantage of the arbitrariness of the regular decomposition dividing lines through the notion of "neighborhood quadrants" (i.e., "softening" the regular decomposition

boundary lines through heuristics for searching neighborhood quadrants for added linkage information) and methods of merging important quadrants to obtain connected areas in the scene in terms of a specific subtree, are given in [36]. We will only repeat here the advantages of regular decomposition as stated in [36]:

1. Via unconditional partitioning, pictures which are physically too big to store in fast memory at one time, can be processed as a sequence of subpictures extracted during preprocessing.
2. Regular decomposition enables addressing for rapid access to any geographical part of the image.
3. Regular decomposition retains explicitly in the data structure a hierarchical description of picture patterns, elements and their relationships. Hence, this scheme may also be used in conjunction with syntactic pattern recognition algorithms [41-44].
4. Representations permit recursive analysis of subpictures.
5. The procedure treats all picture points alike. Hence, it does not prefer objects with any directional orientation or picture location.
6. The decomposition algorithm contains major routines (traversal, tree-creation) which are independent of image class. Small changes can adapt regular decomposition to widely different types of pictures.
7. The resultant tree data structure distinguishes object from non object (or background) and enables processing to locate separate objects.

SECTION 3

BASIC SYMMETRIES AS COMBINATION-CLASSES OF THE TREE'S NODES

3.1 INTRODUCTION

In this section we present the relationships between directional symmetries and the nodes of the picture's tree representation. Two grid points, lying symmetrically opposite with respect to a given line,* constitute a "class" denoted as $S^{\lambda}_{i,j}(\mu)$, where:

- λ : the tree level at which these grid points are found (as we will see below).
- i : the ith "set", to which all classes containing grid points that lie on the same straight line in the picture array belong.
- j : the jth class.
- μ : the direction along which the grid points lie (i.e., along a line perpendicular to the given axis of symmetry).

Each of the above mentioned sets is denoted as $s^{\lambda}_{i}(\mu)$ and contains all classes $S^{\lambda}_{i,j}(\mu)$, j=1,2,3,....

Our initial investigation is restricted to examining classes only along the following principal directions:

1) μ = h : along a horizontal direction (0° or 180°), where we are examining grid points lying symmetrically opposite a vertical line.

---

*Such a line corresponds to an "axis of symmetry", and the two grid points of a pair are equidistant from this axis.

2) $\mu = v$: along a vertical direction (90° or 270°), where we are examining grid points lying symmetrically opposite an horizontal line.

3) $\mu = r$: along the direction of a right-diagonal line (45° or 225°), where we are examining grid points lying symmetrically opposite a left-diagonal line.

4) $\mu = \ell$: along the direction of a left-diagonal line (135° or 315°), where we are examining grid points lying symmetrically opposite a right diagonal line.

In the general case, of course, we may define more directions, thus establishing larger sets of such directional symmetry classes.

In the following paragraphs, we present ways by which these grid points (given as nodes of the corresponding tree) are paired to define various symmetry classes, along the above mentioned four principal directions. We will be referring to square grids of dimensions $2^{\lambda} \times 2^{\lambda}$, where $\lambda = 1,2,3,\ldots,n$. As mentioned before, λ also denotes the tree level. For each of the four main directions, we first present a detailed analysis for $\lambda = 1,2$ and 3 and, then, generalize for the case λ (i.e., for $2^{\lambda} \times 2^{\lambda}$ grids).

3.2 HORIZONTAL SYMMETRY CLASSES ($\mu = h$)

3.2.1 Grid Size: 2x2 (i.e., Level One: $\lambda = 1$)

At this level 1, the original grid P is partitioned into the four equal subgrids P_a, P_b, P_c, P_d of figure 3.1a. The corresponding tree structure of this grid is shown in Figure 3.1b. Each subgrid of Figure 3.1a corresponds to a node of the tree at level 1, or to a "level-1 node".

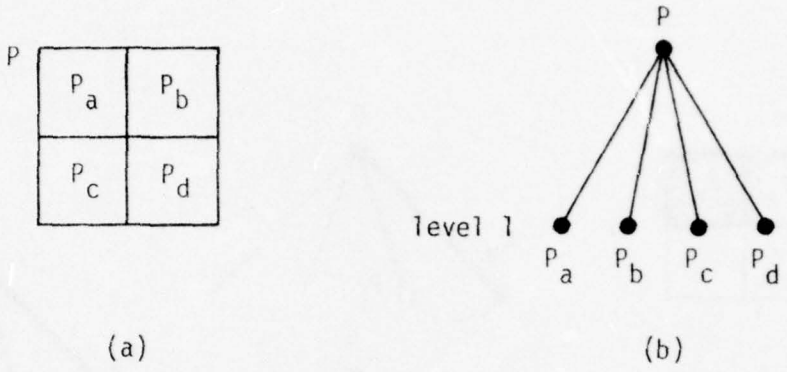

Fig. 3.1: Level 1. (a) The 2 x 2 Grid;
(b) Its Tree Representation.

For the "horizontal symmetry classes" (or "h-symmetry classes", or simply "h-classes"), the picture's grid points are paired as follows:

$$(P_a \text{ with } P_b) \text{ and } (P_c \text{ with } P_d)$$

This is shown on the original picture as the shaded squares of Figure 3.2a, and on its tree representation as the solid lines of Figure 3.2b. Following our notation, each such pair constitutes a symmetry class denoted by $S^1_{i,j}(h)$, where the subscript i distinguishes among the various sets, and the subscript j distinguishes among the various classes.

The resulting h-classes are given (Figure 3.2c) as:

$$\begin{aligned} S^1_{1,1}(h) &= \{P_a , P_b\} \\ S^1_{2,1}(h) &= \{P_c , P_d\} \end{aligned} \tag{3.1}$$

These two classes correspond to the two sets:

$$\begin{aligned} s^1_1(h) &= \{S^1_{1,1}(h)\} \\ s^1_2(h) &= \{S^1_{2,1}(h)\} \end{aligned} \tag{3.2}$$

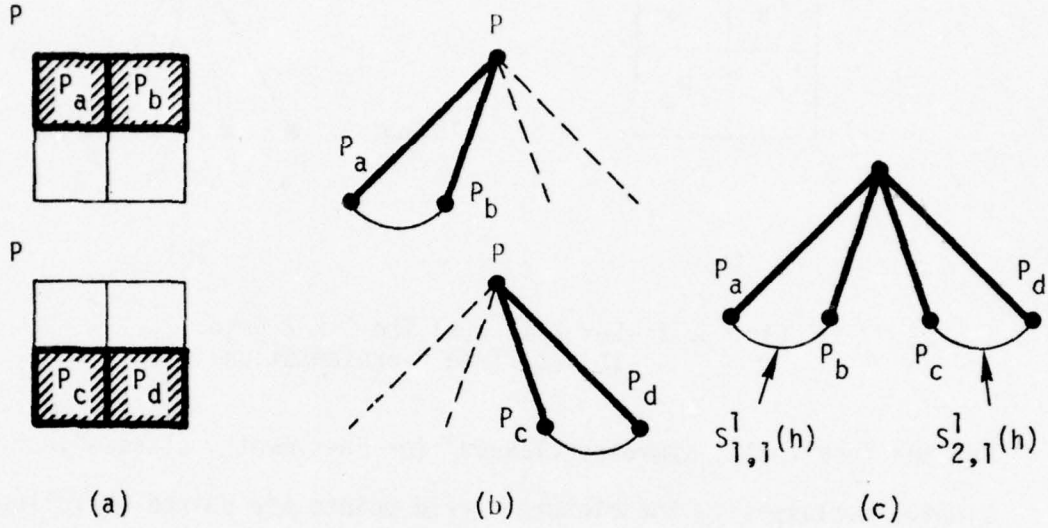

Fig. 3.2: Horizontal Symmetry Classes at Level 1. (a) The Paired Grid Points (Shaded Squares); (b) The Corresponding Paired Nodes of the Tree (Solid Lines); (c) The h-classes.

3.2.2 Grid Size: 4x4 (i.e., Level Two: $\lambda = 2$)

At this level 2, the original grid P is partitioned into the 16 equal subgrids P_{aa}, P_{ab}, ..., P_{dc}, P_{dd} shown in Figure 3.3a. The corresponding tree structure of this grid is shown in Figure 3.3b. Each subgrid of Figure 3.3a corresponds to a node of the tree at level 2 or to a "level-2 node".

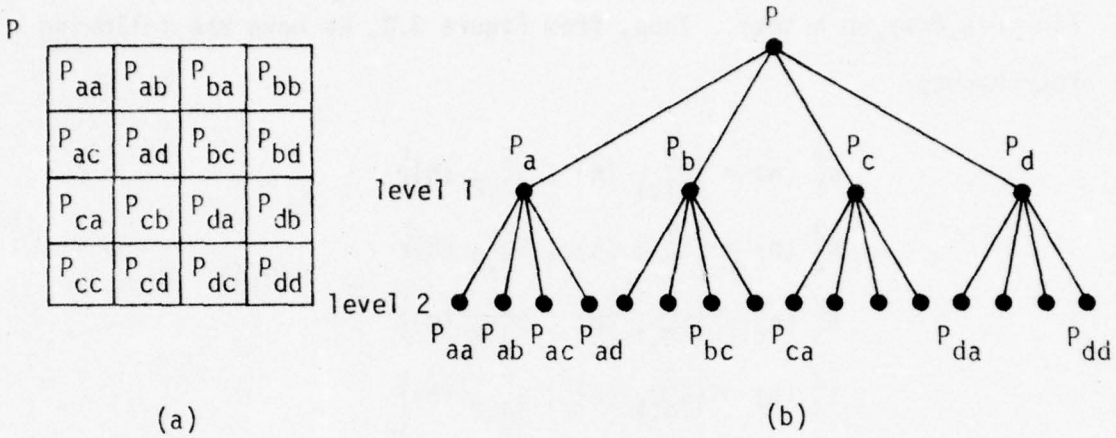

Fig. 3.3: Level 2. (a) The 4 x 4 Grid;
(b) Its Tree Representation.

For the h-classes, the picture's grid-points are paired as follows:

$$(P_{aa} \text{ with } P_{bb}) \text{ and } (P_{ab} \text{ with } P_{ba})$$

$$(P_{ac} \text{ with } P_{bd}) \text{ and } (P_{ad} \text{ with } P_{bc})$$

$$(P_{ca} \text{ with } P_{db}) \text{ and } (P_{cb} \text{ with } P_{da})$$

$$(P_{cc} \text{ with } P_{dd}) \text{ and } (P_{cd} \text{ with } P_{dc})$$

This is shown as the shaded squares of Figure 3.4a or the solid lines of Figure 3.4b. The resulting h-classes are given (Figure 3.4c) as:

$$\begin{aligned}
S^2_{1,1}(h) &= \{P_{aa}, P_{bb}\} \text{ and } S^2_{1,2}(h) = \{P_{ab}, P_{ba}\} \\
S^2_{2,1}(h) &= \{P_{ac}, P_{bd}\} \text{ and } S^2_{2,2}(h) = \{P_{ad}, P_{bc}\} \\
S^2_{3,1}(h) &= \{P_{ca}, P_{db}\} \text{ and } S^2_{3,2}(h) = \{P_{cb}, P_{da}\} \\
S^2_{4,1}(h) &= \{P_{cc}, P_{dd}\} \text{ and } S^2_{4,2}(h) = \{P_{cd}, P_{dc}\}
\end{aligned} \tag{3.3}$$

All classes with equal first subscripts, constitute a set (in this case, an h-set). Thus, from Figure 3.4, we have the following four h-sets:

$$
\begin{aligned}
s_1^2(h) &= \left\{ s_{1,1}^2(h) \, , \, s_{1,2}^2(h) \right\} \\
s_2^2(h) &= \left\{ s_{2,1}^2(h) \, , \, s_{2,2}^2(h) \right\} \\
s_3^2(h) &= \left\{ s_{3,1}^2(h) \, , \, s_{3,2}^2(h) \right\} \\
s_4^2(h) &= \left\{ s_{4,1}^2(h) \, , \, s_{4,2}^2(h) \right\}
\end{aligned}
\qquad (3.4)
$$

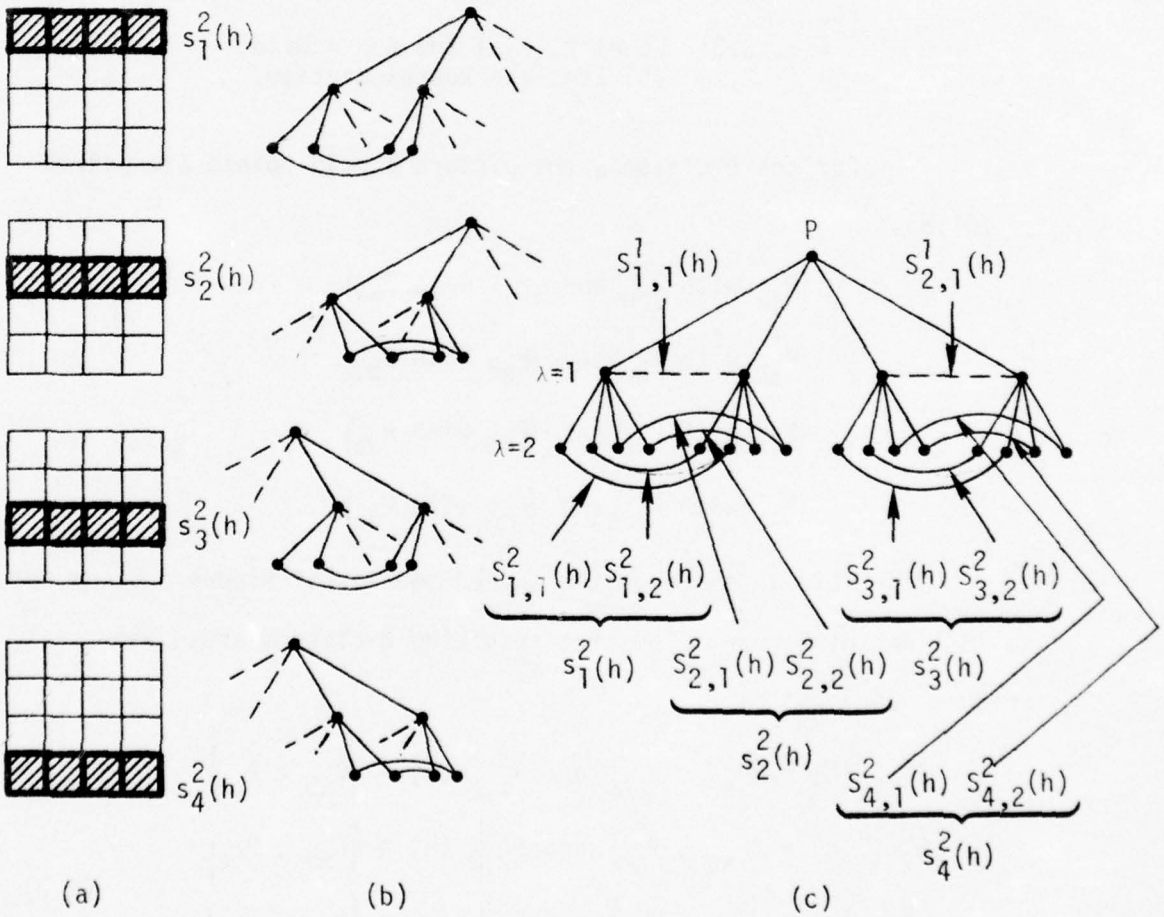

Fig. 3.4: Horizontal Symmetry Classes at Level 2. (a) The Paired Grid-points (Shaded Squares) Which Define Sets; (b) The Corresponding Paired Nodes of the Tree (Solid Lines); (c) The h-classes.

3.2.3 Grid Size: 8x8 (i.e., Level Three: $\lambda = 3$)

At this level, the original grid P is partitioned into the 64 equal subgrids P_{aaa}, P_{aab}, ... , P_{ddd} shown in Figure 3.5a. The corresponding tree structure is shown in Figure 3.5b, where its terminal nodes (leaves) are "level-3 nodes".

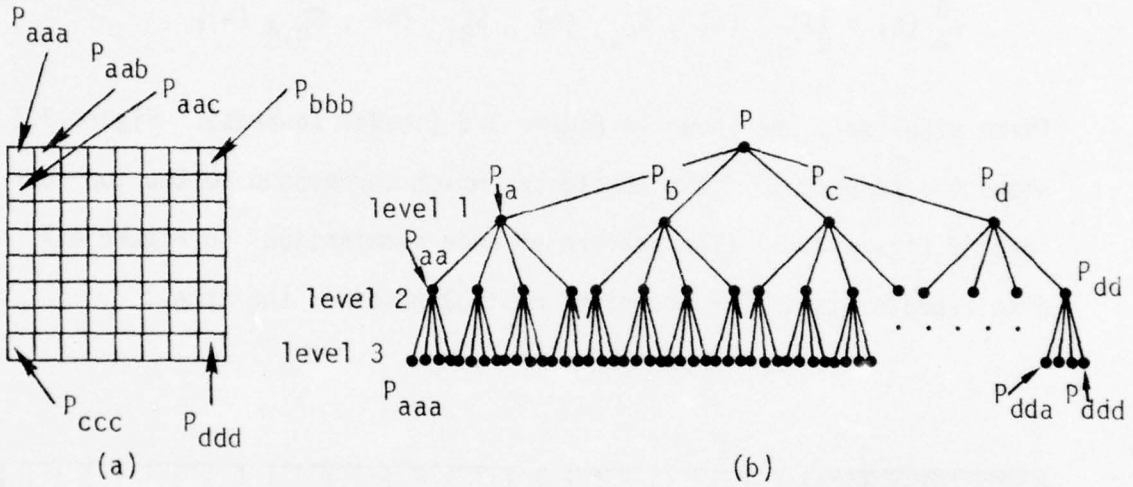

Fig. 3.5: Level 3. (a) The 8 x 8 Grid;
(b) Its Tree Representation.

For the h-classes, there are 32 pairs of the picture's grid points which form the following 32 h-classes:

$$
\begin{array}{|l|l|l|l|}
\hline
S^3_{1,1}(h)=\{P_{aaa},P_{bbb}\} & S^3_{1,2}(h)=\{P_{aab},P_{bba}\} & S^3_{1,3}(h)=\{P_{abb},P_{baa}\} & S^3_{1,4}(h)=\{P_{aba},P_{bab}\} \\
S^3_{2,1}(h)=\{P_{aac},P_{bbd}\} & S^3_{2,2}(h)=\{P_{aad},P_{bbc}\} & S^3_{2,3}(h)=\{P_{abd},P_{bac}\} & S^3_{3,3}(h)=\{P_{abc},P_{bad}\} \\
S^3_{3,1}(h)=\{P_{aca},P_{bdb}\} & S^3_{3,2}(h)=\{P_{acb},P_{bda}\} & S^3_{3,3}(h)=\{P_{adb},P_{bca}\} & S^3_{3,4}(h)=\{P_{ada},P_{bcb}\} \\
S^3_{4,1}(h)=\{P_{acc},P_{bdd}\} & S^3_{4,2}(h)=\{P_{acd},P_{bdc}\} & S^3_{4,3}(h)=\{P_{add},P_{bcc}\} & S^3_{4,4}(h)=\{P_{adc},P_{bcd}\} \\
S^3_{5,1}(h)=\{P_{caa},P_{dbb}\} & S^3_{5,2}(h)=\{P_{cab},P_{dba}\} & S^3_{5,3}(h)=\{P_{cbb},P_{daa}\} & S^3_{5,4}(h)=\{P_{cba},P_{dab}\} \\
S^3_{6,1}(h)=\{P_{cac},P_{dbd}\} & S^3_{6,2}(h)=\{P_{cad},P_{dbc}\} & S^3_{6,3}(h)=\{P_{cbd},P_{dac}\} & S^3_{6,4}(h)=\{P_{cbc},P_{dad}\} \\
S^3_{7,1}(h)=\{P_{cca},P_{ddb}\} & S^3_{7,2}(h)=\{P_{ccb},P_{dda}\} & S^3_{7,3}(h)=\{P_{cdb},P_{dca}\} & S^3_{7,4}(h)=\{P_{cda},P_{dcb}\} \\
S^3_{8,1}(h)=\{P_{ccc},P_{ddd}\} & S^3_{8,2}(h)=\{P_{ccd},P_{ddc}\} & S^3_{8,3}(h)=\{P_{cdd},P_{dcc}\} & S^3_{8,4}(h)=\{P_{cdc},P_{dcd}\} \\
\hline
\end{array}
\qquad (3.5)
$$

These classes form the following eight h-sets:

$$
\begin{aligned}
s_1^3(h) &= \left\{S_{1,1}^3(h),\ S_{1,2}^3(h),\ S_{1,3}^3(h),\ S_{1,4}^3(h)\right\} \\
s_2^3(h) &= \left\{S_{2,1}^3(h),\ S_{2,2}^3(h),\ S_{2,3}^3(h),\ S_{2,4}^3(h)\right\} \qquad (3.6) \\
&\vdots \\
s_8^3(h) &= \left\{S_{8,1}^3(h),\ S_{8,2}^3(h),\ S_{8,3}^3(h),\ S_{8,4}^3(h)\right\}
\end{aligned}
$$

These eight sets are shown in Figure 3.6 (shaded squares). Figure 3.7 shows the respective first 16 classes which correspond to the top four sets of Figure 3.6. (The pattern of node combinations in Figure 4.7 also repeats itself for the right most 32 nodes of the tree.)

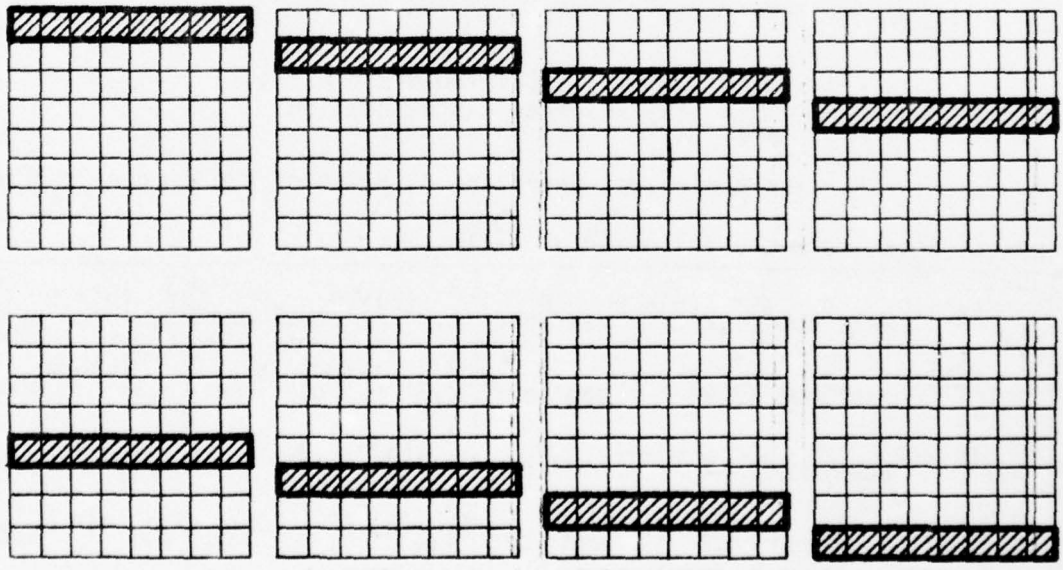

Fig. 3.6: Horizontal Symmetry Classes at Level 3. The Shaded Squares Identify the Eight Different Sets.

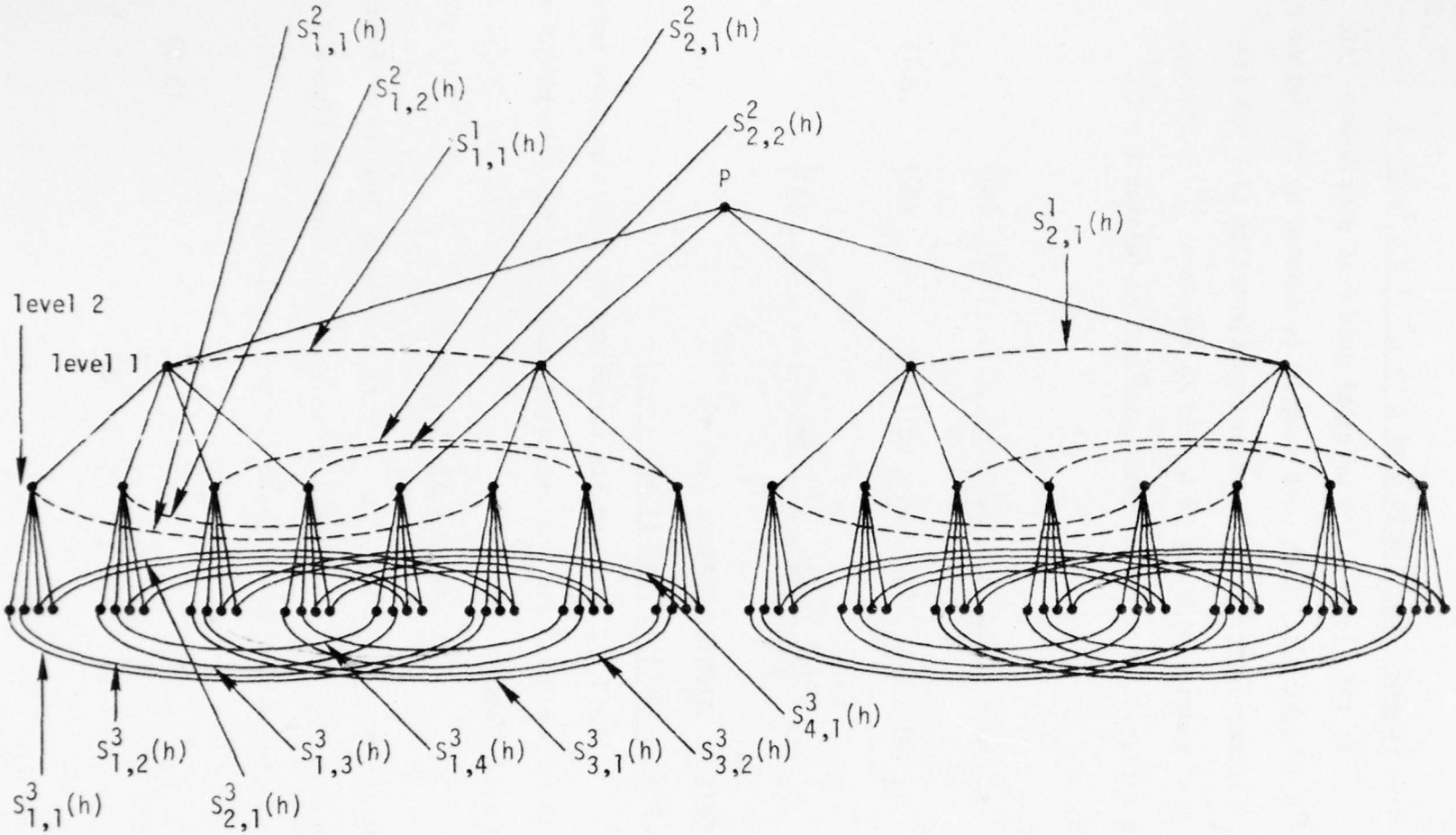

Fig. 3.7: Horizontal Symmetry Classes at Level 3 as Combinations of the Tree Nodes (The Pattern Repeats Itself for the Rightmost 32 Nodes of the Tree.)

3.2.4 General Case: Grid Size $2^\lambda \times 2^\lambda$ (i.e., Level λ)

At this level λ the original grid P is partitioned into $2^\lambda \times 2^\lambda = 4^\lambda$ subgrids. Each such subgrid is denoted by the letter P having λ letter-subscripts. The tree representation of P has (at level λ), 4^λ nodes, which may be paired to form $p = \frac{4^\lambda}{2}$ h-classes. These p h-classes form $k = 2^\lambda$ sets, each set containing $t = 2^{\lambda-1}$ classes:

$$
\begin{aligned}
s_1^\lambda(h) &= \left\{S_{1,1}^\lambda(h)\ ,\ S_{1,2}^\lambda(h)\ ,\ \ldots\ ,\ S_{1,t}^\lambda(h)\right\} \\
s_2^\lambda(h) &= \left\{S_{2,1}^\lambda(h)\ ,\ S_{2,2}^\lambda(h)\ ,\ \ldots\ ,\ S_{2,t}^\lambda(h)\right\} \qquad (3.7) \\
&\ \ \vdots \\
s_k^\lambda(h) &= \left\{S_{k,1}^\lambda(h)\ ,\ S_{k,2}^\lambda(h)\ ,\ \ldots\ ,\ S_{k,t}^\lambda(h)\right\}
\end{aligned}
$$

3.3 VERTICAL SYMMETRY CLASSES ($\mu = v$)

3.3.1 Grid Size: 2x2 (i.e., $\lambda = 1$)

The 2 x 2 grid and its corresponding tree structure were shown in Figure 3.1. For the v-classes, the picture's grid-points are paired as follows:

$$\left(P_a \text{ with } P_c\right) \text{ and } \left(P_b \text{ with } P_d\right)$$

This is shown on the original picture as the shaded squares of Figure 3.8a and on its tree representation as the solid lines of Figure 3.8b. The resulting v-classes are given (Figure 3.8c) as:

$$
\begin{aligned}
S_{1,1}^1(v) &= \left\{P_a\ ,\ P_c\right\} \\
S_{2,1}^1(v) &= \left\{P_b\ ,\ P_d\right\}
\end{aligned}
\qquad (3.8)
$$

These two classes correspond to the two sets:

$$s_1^1(v) = \left\{S_{1,1}^1(v)\right\}$$
$$s_2^1(v) = \left\{S_{2,1}^1(v)\right\} \qquad (3.9)$$

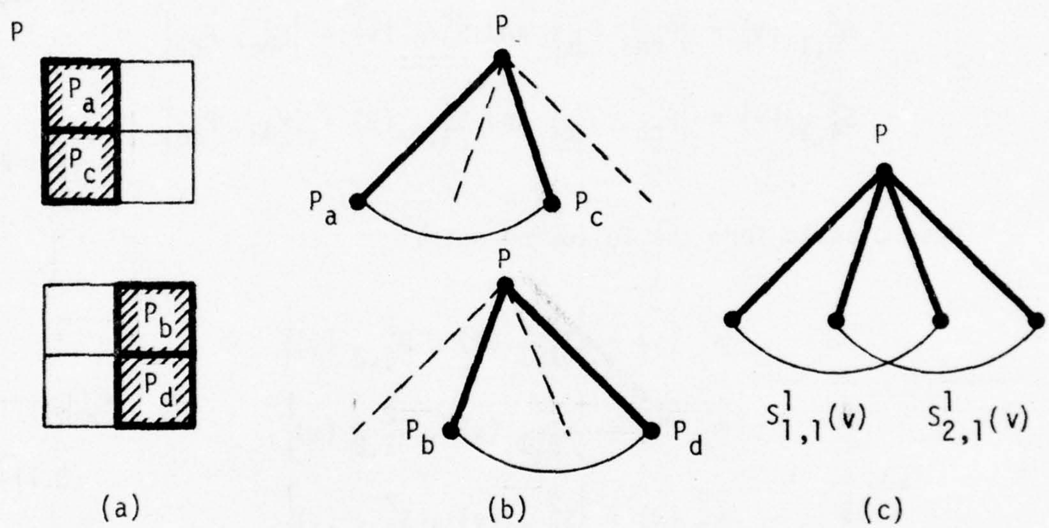

Fig. 3.8: Vertical Symmetry Classes at Level 1. (a) The Paired Grid Points (Shaded Squares); (b) The Corresponding Paired Nodes of the Tree (Solid Lines); (c) The v-classes.

3.3.2 Grid Size: 4x4 (i.e., $\lambda = 2$)

The 4 x 4 grid and its tree representation are the same as the ones shown in Figure 3.3. For the v-classes, the picture's grid-points are paired as follows:

$(P_{aa}$ with $P_{cc})$ and $(P_{ac}$ with $P_{ca})$

$(P_{ab}$ with $P_{cd})$ and $(P_{ad}$ with $P_{cb})$

$(P_{ba}$ with $P_{dc})$ and $(P_{bc}$ with $P_{da})$

$(P_{bb}$ with $P_{dd})$ and $(P_{bd}$ with $P_{db})$

This is shown as the shaded squares of Figure 3.9a or the solid lines of Figure 3.9b. The resulting v-classes are given (Figure 3.9c) as:

$$
\begin{aligned}
S^2_{1,1}(v) &= \{P_{aa}, P_{cc}\} \text{ and } S^2_{1,2}(v) = \{P_{ac}, P_{ca}\} \\
S^2_{2,1}(v) &= \{P_{ab}, P_{cd}\} \text{ and } S^2_{2,2}(v) = \{P_{ad}, P_{cb}\} \\
S^2_{3,1}(v) &= \{P_{ba}, P_{dc}\} \text{ and } S^2_{3,2}(v) = \{P_{bc}, P_{da}\} \\
S^2_{4,1}(v) &= \{P_{bb}, P_{dd}\} \text{ and } S^2_{4,2}(v) = \{P_{bd}, P_{db}\}
\end{aligned}
\tag{3.10}
$$

These classes form the following sets:

$$
\begin{aligned}
s^2_1(v) &= \{S^2_{1,1}(v), S^2_{1,2}(v)\} \\
s^2_2(v) &= \{S^2_{2,1}(v), S^2_{2,2}(v)\} \\
s^2_3(v) &= \{S^2_{3,1}(v), S^2_{3,2}(v)\} \\
s^2_4(v) &= \{S^2_{4,1}(v), S^2_{4,2}(v)\}
\end{aligned}
\tag{3.11}
$$

3.3.3 Grid Size: 8x8 (i.e., $\lambda = 3$)

The 8 x 8 grid and its tree representation are the same as the ones shown in Figure 3.5. For the v-classes, there are 32 pairs of the picture's grid-points which form the following 32 classes:

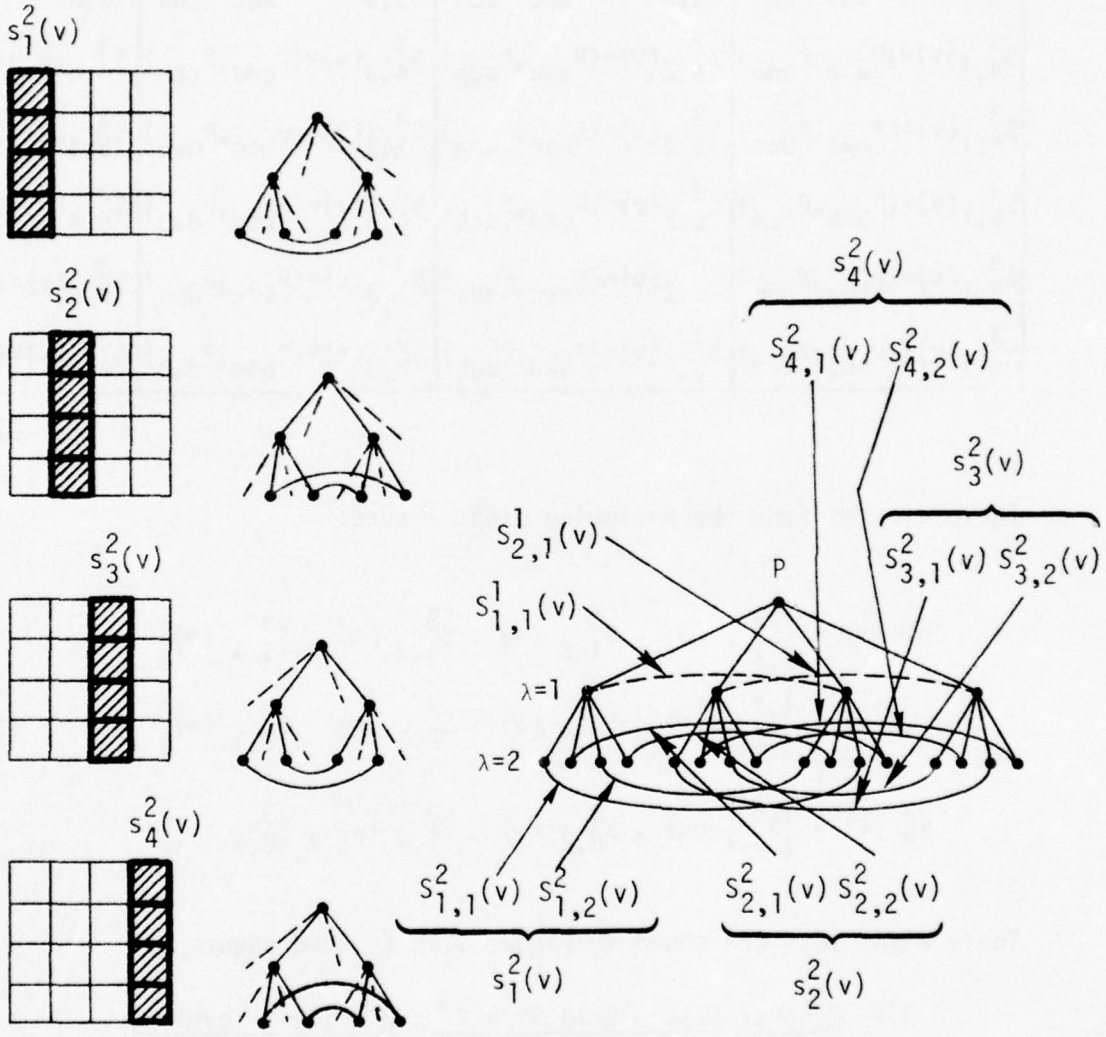

Fig. 3.9: Vertical Symmetry Classes at Level 2. (a) The Paired Grid-points (Shaded Squares) which Define Sets; (b) The Corresponding Paired Nodes of the Tree (Solid Lines); (c) The v-classes.

$S^3_{1,1}(v)=\{P_{aaa},P_{ccc}\}$	$S^3_{1,2}(v)=\{P_{aac},P_{cca}\}$	$S^3_{1,3}(v)=\{P_{acc},P_{caa}\}$	$S^3_{1,4}(v)=\{P_{aca},P_{cac}\}$
$S^3_{2,1}(v)=\{P_{aab},P_{ccd}\}$	$S^3_{2,2}(v)=\{P_{aad},P_{ccb}\}$	$S^3_{2,3}(v)=\{P_{acd},P_{cab}\}$	$S^3_{2,4}(v)=\{P_{acb},P_{cad}\}$
$S^3_{3,1}(v)=\{P_{aba},P_{cdc}\}$	$S^3_{3,2}(v)=\{P_{abc},P_{cda}\}$	$S^3_{3,3}(v)=\{P_{adc},P_{cba}\}$	$S^3_{3,4}(v)=\{P_{ada},P_{cbc}\}$
$S^3_{4,1}(v)=\{P_{abb},P_{cdd}\}$	$S^3_{4,2}(v)=\{P_{abd},P_{cdb}\}$	$S^3_{4,3}(v)=\{P_{add},P_{cbb}\}$	$S^3_{4,4}(v)=\{P_{adb},P_{cbd}\}$
$S^3_{5,1}(v)=\{P_{baa},P_{dcc}\}$	$S^3_{5,2}(v)=\{P_{bac},P_{dca}\}$	$S^3_{5,3}(v)=\{P_{bcc},P_{daa}\}$	$S^3_{5,4}(v)=\{P_{bca},P_{dac}\}$
$S^3_{6,1}(v)=\{P_{bab},P_{dcd}\}$	$S^3_{6,2}(v)=\{P_{bad},P_{dcb}\}$	$S^3_{6,3}(v)=\{P_{bcd},P_{dab}\}$	$S^3_{6,4}(v)=\{P_{bcb},P_{dad}\}$
$S^3_{7,1}(v)=\{P_{bba},P_{ddc}\}$	$S^3_{7,2}(v)=\{P_{bbc},P_{dda}\}$	$S^3_{7,3}(v)=\{P_{bdc},P_{dba}\}$	$S^3_{7,4}(v)=\{P_{bda},P_{dbc}\}$
$S^3_{8,1}(v)=\{P_{bbb},P_{ddd}\}$	$S^3_{8,2}(v)=\{P_{bbd},P_{ddb}\}$	$S^3_{8,3}(v)=\{P_{bdd},P_{dbb}\}$	$S^3_{8,4}(v)=\{P_{bdb},P_{dbd}\}$

(3.12)

These classes form the following eight v-sets:

$$\begin{aligned} s^3_1(v) &= \left\{S^3_{1,1}(v),\ S^3_{1,2}(v),\ S^3_{1,3}(v),\ S^3_{1,4}(v)\right\} \\ s^3_2(v) &= \left\{S^3_{2,1}(v),\ S^3_{2,2}(v),\ S^3_{2,3}(v),\ S^3_{2,4}(v)\right\} \\ &\vdots \\ s^3_8(v) &= \left\{S^3_{8,1}(v),\ S^3_{8,2}(v),\ S^3_{8,3}(v),\ S^3_{8,4}(v)\right\} \end{aligned} \qquad (3.13)$$

These eight sets are shown in Figure 3.10 (shaded squares).

3.3.4 General Case: Grid Size $2^\lambda \times 2^\lambda$ (i.e., Level λ)

The same conclusions apply for the v-symmetries as for the h-symmetries of paragraph 3.2.4. The v-classes form $k=2^\lambda$ sets, each set containing $t=2^{\lambda-1}$ classes:

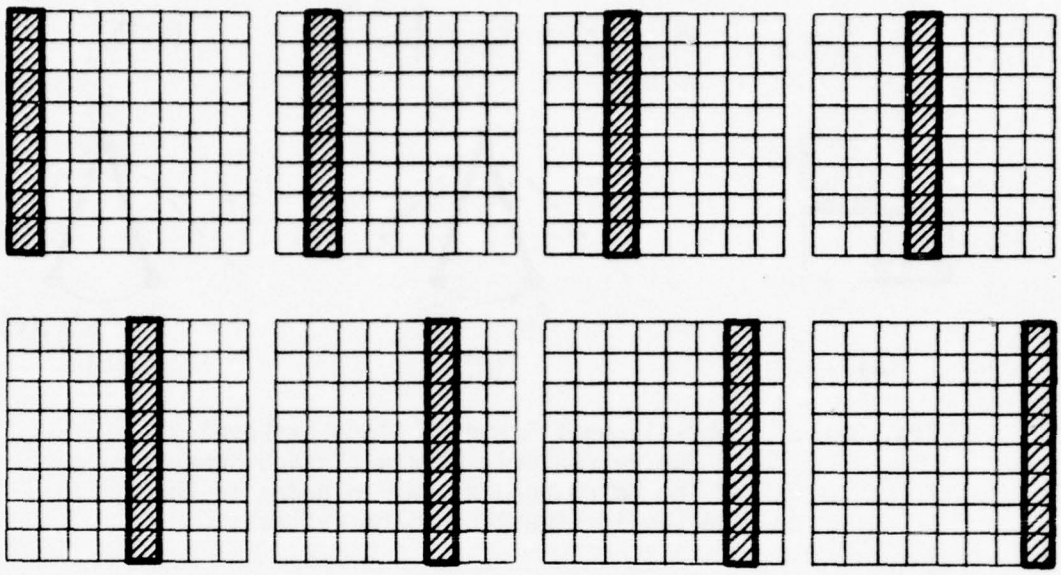

Fig. 3.10: Vertical Symmetry Classes at Level 3. The Shaded Squares Identify the Eight Different Sets.

$$
\begin{aligned}
s_1^{\lambda}(v) &= \left\{ S_{1,1}^{\lambda}(v) \ , \ S_{1,2}^{\lambda}(v), \ \ldots \ , \ S_{1,t}^{\lambda}(v) \right\} \\
s_2^{\lambda}(v) &= \left\{ S_{2,1}^{\lambda}(v) \ , \ S_{2,2}^{\lambda}(v), \ \ldots \ , \ S_{2,t}^{\lambda}(v) \right\} \\
&\vdots \\
s_k^{\lambda}(v) &= \left\{ S_{k,1}^{\lambda}(v) \ , \ S_{k,2}^{\lambda}(v), \ \ldots \ , \ S_{k,t}^{\lambda}(v) \right\}
\end{aligned}
\qquad (3.14)
$$

3.4 RIGHT-DIAGONAL SYMMETRY CLASSES (μ = r)

3.4.1 Grid Size: 2x2 (i.e., λ = 1)

For the r-classes, the picture's grid-points are paired as follows:

$$\left(P_b \text{ with } P_c \right)$$

This is shown in Figure 3.11. The resulting r-class is:

$$S^1_{1,1}(r) = \{P_b, P_c\} \qquad (3.15)$$

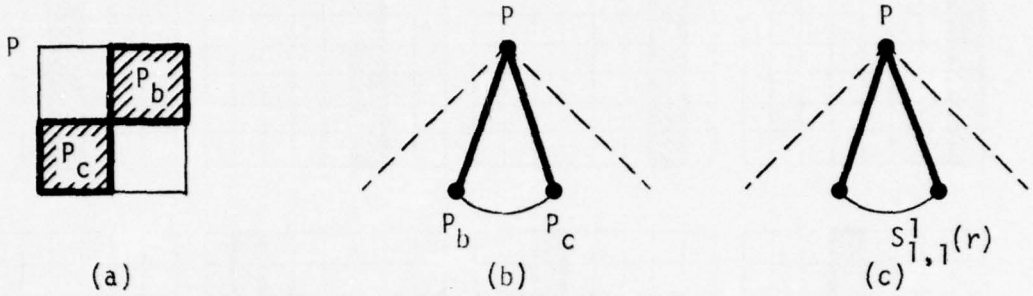

Fig. 3.11: Right-diagonal Symmetry Class at Level 1.
(a) The Paired Grid-Points (Shaded Squares);
(b) The Corresponding Paired Nodes of the Tree (Solid Lines); (c) The r-class.

This class corresponds to the single set:

$$s^1_1(r) = \left\{S^1_{1,1}(r)\right\} \qquad (3.16)$$

3.4.2 Grid Size: 4x4 (i.e., $\lambda = 2$)

For the r-classes, the picture's grid-points are paired as follows:

$(P_{bb}$ with $P_{cc})$ and $(P_{bc}$ with $P_{cb})$

$(P_{ba}$ with $P_{ca})$

$(P_{bd}$ with $P_{cd})$

The resulting r-classes are:

$$S^2_{1,1}(r) = \{P_{bb}, P_{cc}\} \text{ and } S^2_{1,2}(r) = \{P_{bc}, P_{cb}\}$$

$$S^2_{2,1}(r) = \{P_{ba}, P_{ca}\} \qquad (3.17)$$

$$S^2_{3,1}(r) = \{P_{bd}, P_{cd}\}$$

The paired grid-points and tree nodes, as well as these four r-classes, are shown in Figure 3.12.

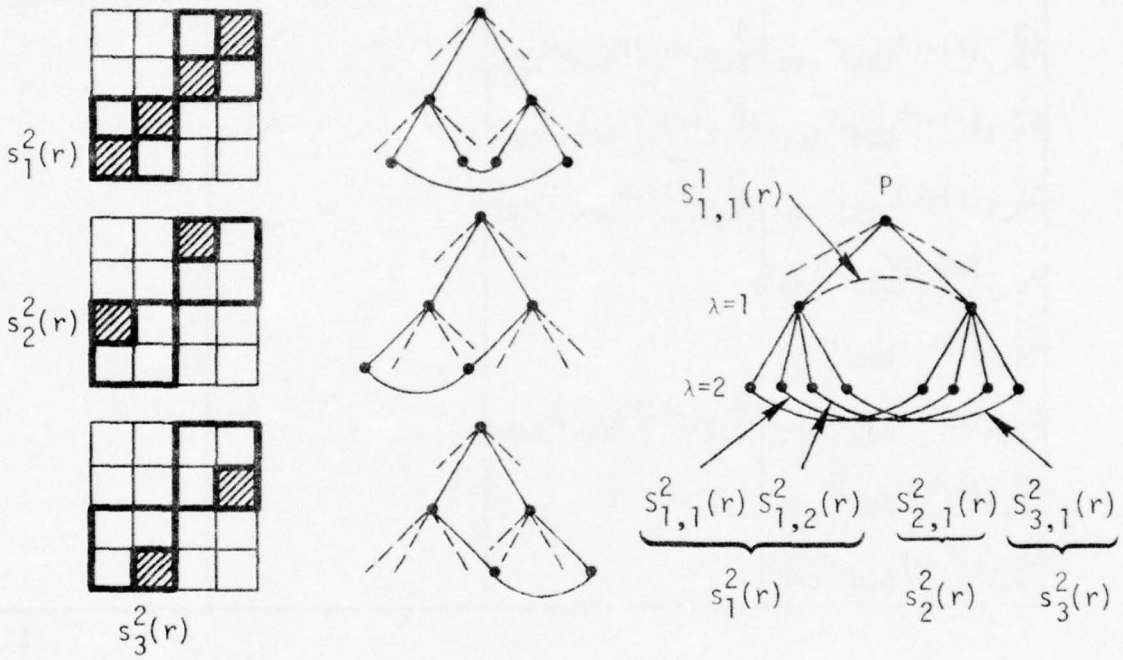

Fig. 3.12: Right-diagonal Symmetry Classes at Level 2. (a) The Paired Grid-Points (Shaded Squares); (b) The Corresponding Paired Nodes of the Tree (Solid Lines); (c) The r-classes.

All classes with equal first subscripts constitute a set (in this case a r-set). Thus, from Figure 3.12, we have the following three r-sets:

$$
\begin{aligned}
s_1^2(r) &= \left\{ s_{1,1}^2(r) \,,\, s_{1,2}^2(r) \right\} \\
s_2^2(r) &= \left\{ s_{2,1}^2(r) \right\} \\
s_3^2(r) &= \left\{ s_{3,1}^2(r) \right\}
\end{aligned}
\qquad (3.18)
$$

3.4.3 Grid Size: 8x8 (i.e., $\lambda = 3$)

For the r-classes, there are 16 pairs of the picture's points (Figure 3.13) which form the following 16 classes:

$S^3_{1,1}(r)=\{P_{bbb},P_{ccc}\}$	$S^3_{1,2}(r)=\{P_{bbc},P_{ccb}\}$	$S^3_{1,3}(r)=\{P_{bcc},P_{cbb}\}$	$S^3_{1,4}(r)=\{P_{bcb},P_{cbc}\}$
$S^3_{2,1}(r)=\{P_{bba},P_{cca}\}$	$S^3_{2,2}(r)=\{P_{bca},P_{cba}\}$		
$S^3_{3,1}(r)=\{P_{bbd},P_{ccd}\}$	$S^3_{3,2}(r)=\{P_{bcd},P_{cbd}\}$		
$S^3_{4,1}(r)=\{P_{bab},P_{cac}\}$	$S^3_{4,2}(r)=\{P_{bac},P_{cab}\}$		
$S^3_{5,1}(r)=\{P_{baa},P_{caa}\}$			
$S^3_{6,1}(r)=\{P_{bad},P_{cad}\}$			
$S^3_{7,1}(r)=\{P_{bdb},P_{cdc}\}$	$S^3_{7,2}(r)=\{P_{bdc},P_{cdb}\}$		
$S^3_{8,1}(r)=\{P_{bda},P_{cda}\}$			
$S^3_{9,1}(r)=\{P_{bdd},P_{cdd}\}$			

(3.19)

The above 16 classes make up the following 9 sets:

$$
\begin{aligned}
s^3_1(r) &= \{S^3_{1,1}(r),\ S^3_{1,2}(r),\ S^3_{1,3}(r),\ S^3_{1,4}(r)\} \\
s^3_2(r) &= \{S^3_{2,1}(r),\ S^3_{2,2}(r)\} \\
s^3_3(r) &= \{S^3_{3,1}(r),\ S^3_{3,2}(r)\} \\
s^3_4(r) &= \{S^3_{4,1}(r),\ S^3_{4,2}(r)\} \qquad (3.20) \\
s^3_5(r) &= \{S^3_{5,1}(r)\} \\
s^3_6(r) &= \{S^3_{6,1}(r)\} \\
s^3_7(r) &= \{S^3_{7,1}(r),\ S^3_{7,2}(r)\} \\
s^3_8(r) &= \{S^3_{8,1}(r)\} \\
s^3_9(r) &= \{S^3_{9,1}(r)\}
\end{aligned}
$$

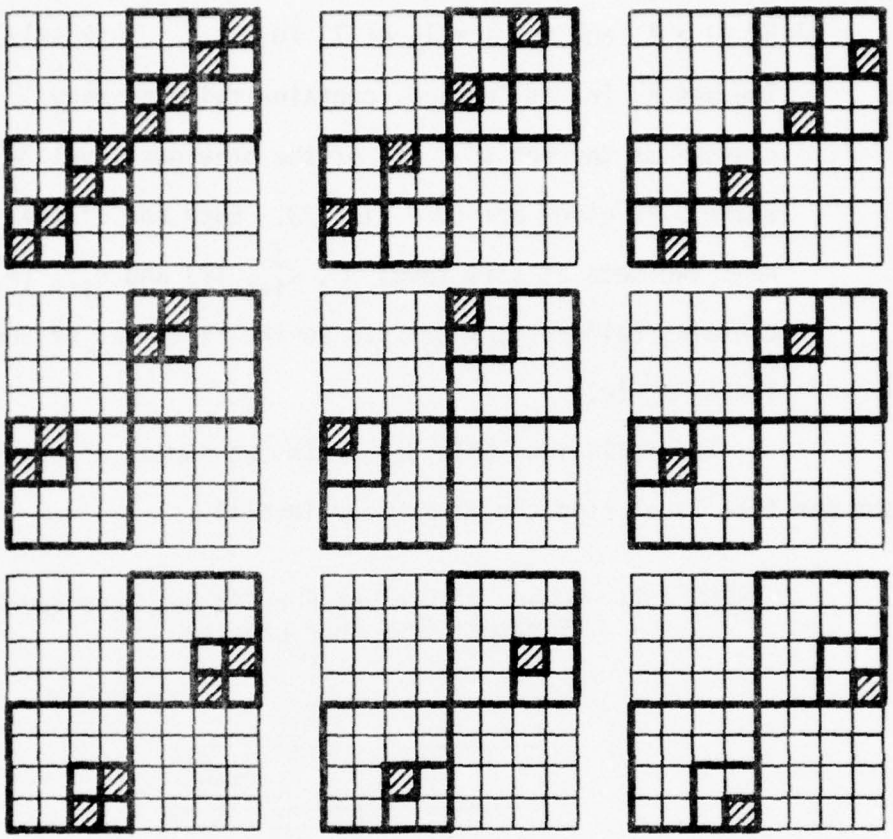

Fig. 3.13: Right-diagonal Symmetry Classes at Level 3. The Shaded Squares Identify the 9 Different Sets.

These 9 sets are shown in Figure 3.13 (shaded squares)

3.4.4 General Case: Grid Size $2^{\lambda} \times 2^{\lambda}$ (i.e., Level λ)

At this level λ, the original grid P is partitioned into 4^{λ} subgrids. The 4^{λ} nodes of the tree (at level λ) are paired to form $q' = 4^{\lambda-1}$ r-classes. These r-classes form $k' = 3^{\lambda-1}$ sets: $s_1^{\lambda}, s_2^{\lambda}, \ldots, s_{k'}^{\lambda}$. The number of classes that each set contains is derived as follows:

a) For $\lambda = 1$, there exists only one set s_1^1 (r), containing only one class $S_{1,1}^1$ (r)

b) For $\lambda > 1$, and for $i = 1, 4, 7, 10, 13, \ldots, (k'-2)$:
The set $s_i^{\lambda}(r)$ at level λ, contains twice as many classes as the set $s_{\sigma}^{\lambda-1}(r)$ of the previous level $\lambda-1$, where σ is given as: $\sigma = (i+2)/3$. Each one of the next two sets at this level λ, $s_{i+1}^{\lambda}(r)$ and $s_{i+2}^{\lambda}(r)$, contains half as many classes as the first set of the level, $s_i^{\lambda}(r)$.

The following Table 3.1 lists the number of classes per set per tree level (for the first four levels).

TABLE 3.1: Number of Classes Per Set Per Tree Level (For the First Four Levels)

Level	Sets	No. of classes per set
$\lambda=1$ ($k'=1$)	$s_1^1(r)$	1
$\lambda=2$ ($k'=3$)	$s_1^2(r)$	2
	$s_2^2(r)$	1
	$s_3^2(r)$	1
$\lambda=3$ $k'=9$	$s_1^3(r)$	4
	$s_2^3(r)$	2
	$s_3^3(r)$	2
	$s_4^3(r)$	2
	$s_5^3(r)$	1
	$s_6^3(r)$	1
	$s_7^3(r)$	2
	$s_8^3(r)$	1
	$s_9^3(r)$	1

Level	Sets	No. of classes per set
$\lambda=4$ ($k'=27$)	$s_1^4(r)$	8
	$s_2^4(r)$	4
	$s_3^4(r)$	4
	$s_4^4(r)$	4
	$s_5^4(r)$	2
	$s_6^4(r)$	2
	$s_7^4(r)$	4
	$s_8^4(r)$	2
	$s_9^4(r)$	2
	$s_{10}^4(r)$	4
	$s_{11}^4(r)$	2
	$s_{12}^4(r)$	2
	$s_{13}^4(r)$	2
	$s_{14}^4(r)$	1
	$s_{15}^4(r)$	1
	$s_{16}^4(r)$	2
	$s_{17}^4(r)$	1
	$s_{18}^4(r)$	1
	$s_{19}^4(r)$	4
	$s_{20}^4(r)$	2
	$s_{21}^4(r)$	2
	$s_{22}^4(r)$	2
	$s_{23}^4(r)$	1
	$s_{24}^4(r)$	1
	$s_{25}^4(r)$	2
	$s_{26}^4(r)$	1
	$s_{27}^4(r)$	1

3.5 LEFT-DIAGONAL SYMMETRY CLASSES ($\mu = \ell$)

3.5.1 Grid Size: 2x2 (i.e., $\lambda = 1$)

For the ℓ-classes at this level, the picture's grid-points are paired as follows:

$$\left(P_a \text{ with } P_d\right)$$

This is shown in Figure 3.14. The resulting ℓ-class is:

$$S^1_{1,1}(\ell) = \left\{P_a\ ,\ P_d\right\} \tag{3.21}$$

This class corresponds to the single ℓ-set:

$$s^1_1(\ell) = \left\{S^1_{1,1}(\ell)\right\} \tag{3.22}$$

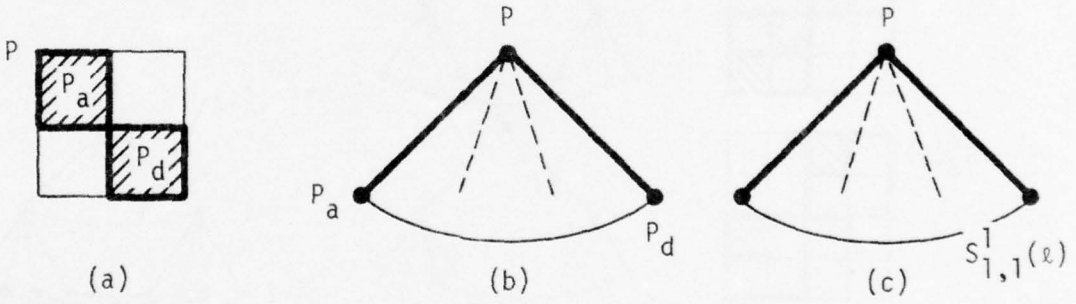

Fig. 3.14: Left-diagonal Symmetry Class at Level 1.
(a) The Paired Grid-points (Shaded Squares);
(b) The Corresponding Paired Nodes of the Tree (Solid Lines); (c) The ℓ-class.

3.5.2 Grid Size: 4x4 (i.e., $\lambda = 2$)

For the ℓ-classes at this level, the picture's grid-points are paired as follows:

$$\left(P_{aa} \text{ with } P_{dd}\right) \text{ and } \left(P_{ad} \text{ with } P_{da}\right)$$

$$\left(P_{ab} \text{ with } P_{db}\right)$$

$$\left(P_{ac} \text{ with } P_{dc}\right)$$

The resulting ℓ-classes are:

$$S^2_{1,1}(\ell) = \{P_{aa}, P_{dd}\} \quad S^2_{1,2}(\ell) = \{P_{ad}, P_{da}\}$$

$$S^2_{2,1}(\ell) = \{P_{ab}, P_{db}\} \tag{3.23}$$

$$S^2_{3,1}(\ell) = \{P_{ac}, P_{dc}\}$$

The paired grid-points and tree nodes, as well as these four ℓ-classes, are shown in Figure 3.15.

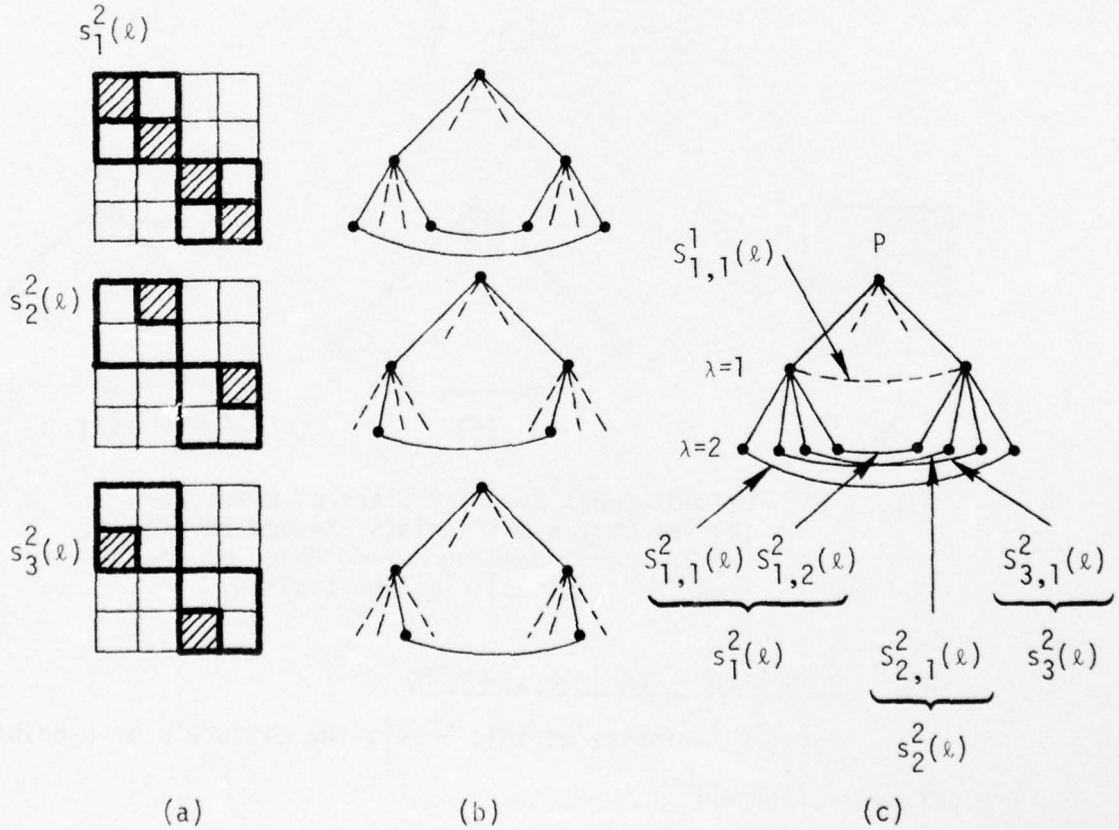

Fig. 3.15: Left-diagonal Symmetry Classes at Level 2. (a) The Paired Grid-points (Shaded Squares); (b) The Corresponding Paired Nodes of the Tree (Solid Lines); (c) The ℓ-classes.

The above four classes form the following three ℓ-sets:

$$s_1^2(\ell) = \{S_{1,1}^2(\ell),\ S_{1,2}^2(\ell)\}$$
$$s_2^2(\ell) = \{S_{2,1}^2(\ell)\} \qquad (3.24)$$
$$s_3^2(\ell) = \{S_{3,1}^2(\ell)\}$$

3.5.3 Grid Size: 8x8 (i.e., $\lambda = 3$)

For the ℓ-classes at this level, there are 16 pairs of the picture's points (Figure 3.16) forming the following 16 classes:

$S_{1,1}^3(\ell)=\{P_{aaa},P_{ddd}\}$	$S_{1,2}^3(\ell)=\{P_{aad},P_{dda}\}$	$S_{1,3}^3(\ell)=\{P_{add},P_{daa}\}$	$S_{1,4}^3(\ell)=\{P_{ada},P_{dad}\}$
$S_{2,1}^3(\ell)=\{P_{aab},P_{ddb}\}$	$S_{2,2}^3(\ell)=\{P_{adb},P_{dab}\}$		
$S_{3,1}^3(\ell)=\{P_{aac},P_{ddc}\}$	$S_{3,2}^3(\ell)=\{P_{dac},P_{adc}\}$		
$S_{4,1}^3(\ell)=\{P_{aba},P_{dbd}\}$	$S_{4,2}^3(\ell)=\{P_{dba},P_{abd}\}$		
$S_{5,1}^3(\ell)=\{P_{abb},P_{dbb}\}$			
$S_{6,1}^3(\ell)=\{P_{abc},P_{dbc}\}$			
$S_{7,1}^3(\ell)=\{P_{aca},P_{dcd}\}$	$S_{7,2}^3(\ell)=\{P_{acd},P_{dca}\}$		
$S_{8,1}^3(\ell)=\{P_{acb},P_{dcb}\}$			
$S_{9,1}^3(\ell)=\{P_{acc},P_{dcc}\}$			

(3.25)

The above 16 classes make up the following 9 sets:

$$
\begin{aligned}
s_1^3(\ell) &= \{s_{1,1}^3(\ell),\ s_{1,2}^3(\ell),\ s_{1,3}^3(\ell),\ s_{1,4}^3(\ell)\} \\
s_2^3(\ell) &= \{s_{2,1}^3(\ell),\ s_{2,2}^3(\ell)\} \\
s_3^3(\ell) &= \{s_{3,1}^3(\ell),\ s_{3,2}^3(\ell)\} \\
s_4^3(\ell) &= \{s_{4,1}^3(\ell),\ s_{4,2}^3(\ell)\} \\
s_5^3(\ell) &= \{s_{5,1}^3(\ell)\} \\
s_6^3(\ell) &= \{s_{6,1}^3(\ell)\} \\
s_7^3(\ell) &= \{s_{7,1}^3(\ell),\ s_{7,2}^3(\ell)\} \\
s_8^3(\ell) &= \{s_{8,1}^3(\ell)\} \\
s_9^3(\ell) &= \{s_{9,1}^3(\ell)\}
\end{aligned}
\tag{3.26}
$$

These 9 sets are shown in Figure 3.16 (shaded squares).

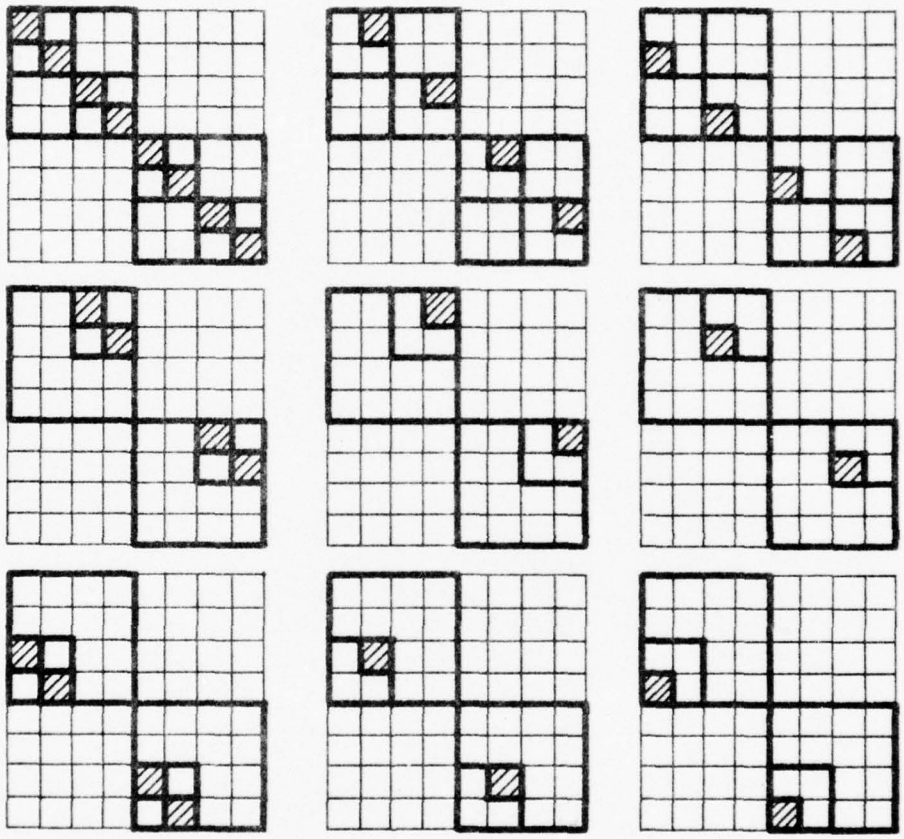

Fig. 3.16: Left-diagonal Symmetry Classes at Level 3. The Shaded Squares Identify the 9 Different Sets.

3.5.4 General Case: Grid Size $2^{\lambda} \times 2^{\lambda}$ (i.e., Level λ)

The same as in Paragraph 3.4.4 for the r-classes. Table 3.1 is still valid, except that for each set, the r is being replaced by ℓ.

SECTION 4

IDENTIFICATION OF SYMMETRY SETS THROUGH A RECURSIVE TRAVERSING OF THE TREE

4.1 INTRODUCTION

The analysis of the previous Section clearly shows that there are certain patterns which repeat themselves as we climb down the tree (i.e. increase the picture resolution by looking into finer details). Furthermore, these patterns remain fixed, and unique to the examined directional symmetry.

Formalizing the above analysis, we present in this section a proposition for developing a recursive algorithm for systematically traversing the tree data-structure to identify directional symmetries. The results obtained include the identification of tree nodes that must be paired (or compared) at each tree level, for each of the above mentioned four directional symmetries.

The algorithm is checked by applying it to the same structured data of the previous section. The results - given in tabular form, at various tree levels, for each of the four symmetries - are the same with the ones obtained with the analysis of Section 3.

4.2 A PROPOSITION

From the analysis of Section 3 we can now derive a recursive algorithm for identifying the tree nodes (grid points or subregions

of the picture) that are paired to define the various symmetry classes, at any level λ of the picture decomposition.

Given any level λ-1, let $s_i^{\lambda-1}$ be one of the sets at this level containing, say, ρ classes: $S_{i,1}^{\lambda-1}$, $S_{i,2}^{\lambda-1}$, $S_{i,3}^{\lambda-1}$, ..., $S_{i,\rho}^{\lambda-1}$. Each class $S_{i,m}^{\lambda-1}$ links two nodes at level λ-1 of the picture's tree representation, i.e. the class is defined generally as:

$$S_{i,m}^{\lambda-1} = \left\{ x_{i,m}^{1},\ x_{i,m}^{2} \right\} \tag{4.1}$$

The first subscript of node x corresponds to the set to which this class belongs, the second subscript to the class in the set, and the superscript is used to distinguish between the two nodes.

From the results of the previous section and for each set $s_i^{\lambda-1}$, we have - at the next higher level of refinement λ - the following:

a) For horizontal or vertical symmetries, there are at most two new sets

$$s_{\gamma_1}^{\lambda}(\cdot) \quad \text{and} \quad s_{\gamma_2}^{\lambda}(\cdot)$$

where the subscripts γ_1 and γ_2 distinguish between the two sets, and $\cdot$ stands for h or u. Furthermore, each such set contains $t = 2^{\lambda-1}$ classes, as pointed out in paragraphs 3.2.4 and 3.3.4.

b) For right-diagonal or left-diagonal symmetries, there are at most three new sets

$$s_{\gamma_1}^{\lambda}(\cdot), \quad s_{\gamma_2}^{\lambda}(\cdot) \quad \text{and} \quad s_{\gamma_3}^{\lambda}(\cdot)$$

where $\cdot$ stands for r or ℓ. The number of classes that each

set contains was derived in paragraphs 3.4.4 and 3.5.4. Using the information of the previous level λ-1, we can easily identify what will the forms be for the sets and classes at this new level of refinement λ. This means that for each symmetry type we can identify the paired nodes which form the respective symmetry classes, and the classes that make up the various sets.

Each class belonging to these "new" sets at level λ, has the general form

$$S^{\lambda}_{i,j} = \{wf_1, w' f_2\} \tag{4.2}$$

i.e. it links two nodes, wf_1 and $w' f_2$. The variables w, w', f_1, and f_2 are defined as follows:

A) The variables w and w' are defined using the data available from the previous level λ-1 and take on the foloowing values:

$$\left.\begin{array}{l} \text{i)} \quad w = x^1_{i,m}, \quad w' = x^2_{i,m} \\ \text{and ii)} \quad w = x^2_{i,m}, \quad w' = x^1_{i,m} \end{array}\right\} \quad \text{for all } m = 1,2,\ldots,\rho \tag{4.3}$$

Therefore, for each class $S^{\lambda-1}_{i,m}$ linking at the previous level λ-1 two nodes $x^1_{i,m}$ and $x^2_{i,m}$, two new different classes are generated at the next higher level of refinement λ, having (from eqs. 4.2 and 4.3) the forms:

$$S^{\lambda}_{i,1} = \{x^1_{i,m} f_1, x^2_{i,m} f_2\} \tag{4.4}$$

$$\text{and} \quad S^{\lambda}_{i,2} = \{x^2_{i,m} f_1, x^1_{i,m} f_2\} \tag{4.5}$$

B) The variables f_1 and f_2 take on different values according to the respective symmetry type under consideration. For the four symmetries we have the following:

B1) For h-symmetries:

As mentioned above, for each set $s_i^{\lambda-1}(h)$ of the previous level λ-1 there are at most two new sets $s_{\gamma_1}^{\lambda}(h)$ and $s_{\gamma_2}^{\lambda}(h)$ at the new level λ, each containing t classes.

Each h-class of the first new set $s_{\gamma_1}^{\lambda}(h)$ has

$$f_1 = a \quad \text{and} \quad f_2 = b \tag{4.6}$$

and, therefore from eq. 4.2, its general form becomes:

$$s_{\gamma_1,j}^{\lambda}(h) = \{wa,\ w'b\} \qquad \text{for all } m=1,2,\ldots,\rho \tag{4.7}$$

On the other hand, each h-class of the second new set $s_{\gamma_2}^{\lambda}(h)$ has

$$f_1 = c \quad \text{and} \quad f_2 = d \tag{4.8}$$

and, therefore, its general form becomes:

$$s_{\gamma_2,j}^{\lambda}(h) = \{wc,\ w'd\} \qquad \text{for all } m=1,2,\ldots,\rho \tag{4.9}$$

B2) For v-symmetries:

Again, there are at most two new sets $s_{\gamma_1}^{\lambda}(v)$ and $s_{\gamma_2}^{\lambda}(v)$ at level λ, each containing t classes. Each v-class of the first new set $s_{\gamma_1}^{\lambda}(v)$ has

$$f_1 = a \quad \text{and} \quad f_2 = c \tag{4.10}$$

and, therefore, its general form becomes:

$$S^{\lambda}_{\gamma_1,j}(v) = \{wa,\ w'c\} \qquad \text{for all } m=1,2,\ldots,\rho \qquad (4.11)$$

Each v-class of the second new set $s^{\lambda}_{\gamma_2}(v)$ has

$$f_1 = b \quad \text{and} \quad f_2 = d \qquad (4.12)$$

and, therefore, its general form becomes:

$$S^{\lambda}_{\gamma_2,j}(v) = \{wb,\ w'd\} \qquad \text{for all } m=1,2,\ldots,\rho \qquad (4.13)$$

B3) For r-symmetries:

Here, for each $s^{\lambda-1}_{i}(r)$, there are at most three new sets $s^{\lambda}_{\gamma_1}(r)$, $s^{\lambda}_{\gamma_2}(r)$, and $s^{\lambda}_{\gamma_3}(r)$, each containing the number of classes derived in Paragraph 3.4.4.

Each r-class of the first new set $s^{\lambda}_{\gamma_1}(r)$ has

$$f_1 = b \quad \text{and} \quad f_2 = c \qquad (4.14)$$

and, therefore, its general form becomes:

$$S^{\lambda}_{\gamma_1,j}(r) = \{wb,\ w'c\} \qquad \text{for all } m=1,2,\ldots,\rho \qquad (4.15)$$

Each class of the second new set $s^{\lambda}_{\gamma_2}(r)$ has

$$f_1 = f_2 = a \qquad (4.16)$$

and, therefore, its general form becomes:

$$S^{\lambda}_{\gamma_2,j}(r) = \{wa,\ w'a\} \qquad \text{for all } m=1,2,\ldots,\rho \qquad (4.17)$$

Finally, each class of the third new set $s^{\lambda}_{\gamma_3}(r)$ has

$$f_1 = f_2 = d \qquad (4.18)$$

and, therefore, its general form becomes:

$$S^{\lambda}_{\gamma_3,j}(r) = \{wd,\ w'd\} \qquad \text{for all } m=1,2,\ldots,\rho \qquad (4.19)$$

B4) For ℓ-symmetries:

Again, there are at most three new sets $s^{\lambda}_{\gamma_1}(\ell)$, $s^{\lambda}_{\gamma_2}(\ell)$, and $s^{\lambda}_{\gamma_3}(\ell)$, each containing the number of classes derived in Paragraph 3.5.4.

Each class of the first new set $s^{\lambda}_{\gamma_1}(\ell)$ has

$$f_1 = a \quad \text{and} \quad f_2 = d \qquad (4.20)$$

and, therefore, its general form becomes:

$$S^{\lambda}_{\gamma_1,j}(\ell) = \{wa,\ w'd\} \qquad \text{for all } m=1,2,\ldots,\rho \qquad (4.21)$$

Each class of the second new set $s^{\lambda}_{\gamma_2}(\ell)$ has

$$f_1 = f_2 = b \qquad (4.22)$$

and, therefore, its general form becomes:

$$S^{\lambda}_{\gamma_2,j}(\ell) = \{wb,\ w'b\} \qquad \text{for all } m=1,2,\ldots,\rho \qquad (4.23)$$

Finally, each class of the third new set $s^{\lambda}_{\gamma_3}(\ell)$ has

$$f_1 = f_2 = c \qquad (4.24)$$

and, therefore, its form becomes

$$S^{\lambda}_{\gamma_3,j}(\ell) = \{wc,\ w'c\} \qquad \text{for all } m=1,2,\ldots,\rho \qquad (4.25)$$

The above cases B1, B2, B3, B4 are shown graphically in Figure 4.1. For example, for h-symmetries the values that f_1 and f_2 take on

are, (a and b) or (c and d); for ℓ-symmetries the values are (a and d) or (b and b) or (c and c), etc.

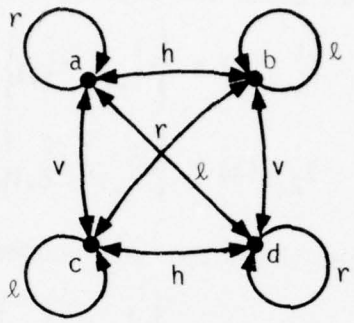

Fig. 4.1: Graphical Representation of the Values that f_1 and f_2 Have for the Four Different Symmetries (h,v,r,ℓ).

4.3 EXAMPLES

Using the above proposition we now give a few examples for the recursive identification of the classes at the next higher level of refinement.

4.3.1 Level 1 (i.e., $\lambda = 1$)

This is the first level of refinement, where a picture P is decomposed into the four subpictures Pa, Pb, Pc, and Pd, and from which all recursive definitions start. At level $\lambda = 1$, there are at most two possible sets, each containing $t = 1$ symmetry-class. Therefore, at this level, a set is equivalent to a class, having the general forms:

$$s_1^1(\cdot) = S_{1,1}^1(\cdot) = \left\{x_{1,1}^1,\ x_{1,1}^2\right\} \qquad (4.26)$$

$$\text{and} \quad s_2^1(\cdot) = S_{2,1}^1(\cdot) = \left\{x_{2,1}^1,\ x_{2,1}^2\right\} \tag{4.27}$$

For h-symmetries these two sets become:

$$s_1^1(h) = S_{1,1}^1(h) = \left\{x_{1,1}^1,\ x_{1,1}^2\right\} = \left\{Pa,\ Pb\right\} \tag{4.28}$$

$$s_2^1(h) = S_{2,1}^1(h) = \left\{x_{2,1}^1,\ x_{2,1}^2\right\} = \left\{Pc,\ Pd\right\} \tag{4.29}$$

For v-symmetries these two sets become:

$$s_1^1(v) = S_{1,1}^1(v) = \left\{x_{1,1}^1,\ x_{1,1}^2\right\} = \left\{Pa,\ Pc\right\} \tag{4.30}$$

$$s_2^1(v) = S_{2,1}^1(v) = \left\{x_{2,1}^1,\ x_{2,1}^2\right\} = \left\{Pb,\ Pd\right\} \tag{4.31}$$

For r-symmetries there is one set:

$$s_1^1(r) = S_{1,1}^1(r) = \left\{x_{1,1}^1,\ x_{1,1}^2\right\} = \left\{Pb,\ Pc\right\} \tag{4.32}$$

For ℓ-symmetries there is also one set:

$$s_1^1(\ell) = S_{1,1}^1(\ell) = \left\{x_{1,1}^1,\ x_{1,1}^2\right\} = \left\{Pa,\ Pd\right\} \tag{4.33}$$

4.3.2 Level 2 (i.e., $\lambda = 2$)

4.3.2.1 h-symmetries

Using the data available at the previous level $\lambda = 1$ (eqs. 4.28 and 4.29) we have $x_{1,1}^1 = Pa$, $x_{1,1}^2 = Pb$, $x_{2,1}^1 = Pc$, and $x_{2,1}^2 = Pd$, which will be used to identify the paired tree nodes for the h-symmetry classes at this higher level of refinement $\lambda = 2$.

At this new level of refinement, from the proposition of Paragraph 4.2, for each of the two sets $s_1^1(h)$ and $s_2^1(h)$ of eqs. 4.12 and 4.13 we have at most two new sets $s_{\gamma_1}^2(h)$ and $s_{\gamma_2}^2(h)$, each containing

$t = 2^{2-1} = 2$ classes.

Using the proposition, we will now define all classes (i.e., the pair of nodes linked by each class) and all sets (i.e., the classes that each set contains) at level 2. Since there are two sets $s_1^1(h)$ and $s_2^1(h)$ at the previous level 1, our procedure is subdivided into two parts: one starting with the classes of the first set $s_1^1(h)$ and the other starting with the classes of the second set $s_2^1(h)$.

1) Using the first "old" set $s_1^1(h)$:

From eq. 4.28 the "old" set contains only one class $S_{1,1}^1(h)$ (second column of Table 4.1a) linking the two nodes Pa and Pb. Therefore, $x_{1,1}^1$ = Pa and $x_{1,1}^2$ = Pb (third column of Table 4.1a). The variables w and w' needed to identify the classes at this new level of refinement 2 (see eq. 4.2) are defined from eq. 4.3 as shown in the fourth column of Table 4.1a. At the present level of refinement $\lambda = 2$,

Table 4.1a: h-symmetry Classes at $\lambda = 2$.
[Starting with $s_1^1(h)$]

Previous level (λ=1)				Present level (λ=2)	
m	Classes of "old" set	Node pairs	Variables w and w'	Classes of the first "new" set $s_1^2(h)$: $S_{1,j}^2(h)$={wa,w'b}	Classes of the second "new" set $s_2^2(h)$: $S_{2,j}^2(h)$={wc, w'd}
1	$S_{1,1}^1(h)$	$x_{1,1}^1$=Pa	w=$x_{1,1}^1$, w'=$x_{1,1}^2$	$S_{1,1}^2(h)$={Paa,Pbb}	$S_{2,1}^2(h)$={Pac,Pbd}
		$x_{1,1}^2$=Pb	w=$x_{1,1}^2$, w'=$x_{1,1}^1$	$S_{1,2}^2(h)$={Pba,Pab}	$S_{2,2}^2(h)$={Pbc,Pad}

there are at most two "new" sets - denoted as $s_1^2(h)$ and $s_2^2(h)$ - each containing two classes which, from the proposition eqs. 4.7 and 4.8, will have the respective general forms:

$$S_{1,j}^2(h) = \{wa,\ w'b\} \quad , \quad j=1,2$$

and (4.34)

$$S_{2,j}^2(h) = \{wc,\ w'd\} \quad , \quad j=1,2$$

where the variable w and w' are defined as in column 4 of Table 4.1a. The resulting "new" classes at the present level $\lambda = 2$ are given in the fifth and sixth columns of Table 4.1a. The first column of Table 4.1a shows all the values that m takes, i.e. m = 1, 2, ..., p. Therefore, using information available at the previous level $\lambda = 1$, and starting with the first "old" set $s_1^1(h)$ we have defined each class of the two "new" sets $s_1^2(h)$ and $s_2^2(h)$ at the present level $\lambda = 2$.

2) Using the second "old" set $s_2^1(h)$:

From eq. 4.29 the "old" set contains only one class $S_{2,1}^1(h)$ (second column of Table 4.1b) linking the two nodes Pc and Pd. Therefore, $x_{2,1}^1$ = Pc and $x_{2,1}^2$ = Pd (third column of Table 4.1b). The variables w and w' are defined from eq. 4.3 as shown in the fourth column of Table 4.1b. The two "new" sets of the present level $\lambda = 2$ are denoted as $s_3^2(h)$ and $s_4^2(h)$, and each contains two classes whose general forms are as in eq. 4.34 above. These classes are

shown in the fifth and sixth columns of Table 4.1b.

Table 4.1b: h-symmetry Classes at $\lambda = 2$.
[Starting with $s_2^1(h)$]

Previous level (λ=1)				Present level (λ=2)	
m	Classes of "old" set	Node pairs	Variables w and w'	Classes of the first "new" set $s_3^2(h)$: $S_{3,j}^2(h)$={wa,w'b}	Classes of the second "new" set $s_4^2(h)$: $S_{4,j}^2(h)$={wc, w'd}
1	$S_{2,1}^1(h)$	$x_{2,1}^1$=Pc	$w=x_{2,1}^1$, $w'=x_{2,1}^2$	$S_{3,1}^2(h)$={Pca,Pdb}	$S_{4,1}^2(h)$={Pcc,Pdd}
		$x_{2,1}^2$=Pd	$w=x_{2,1}^2$, $w'=x_{2,1}^1$	$S_{3,2}^2(h)$={Pda,Pcb}	$S_{4,2}^2(h)$={Pdc,Pcd}

Thus, for the h-symmetries at level 2, we have the following four sets of classes:

$$s_1^2(h) = \left\{S_{1,1}^2(h),\ S_{1,2}^2(h)\right\}$$

$$s_2^2(h) = \left\{S_{2,1}^2(h),\ S_{2,2}^2(h)\right\}$$

$$s_3^2(h) = \left\{S_{3,1}^2(h),\ S_{3,2}^2(h)\right\}$$

$$s_4^2(h) = \left\{S_{4,1}^2(h),\ S_{4,2}^2(h)\right\} \qquad (4.35)$$

Equation 4.35 is the same as eq. 3.4 of Section 3. The classes in eq. 4.35 are as defined in Tables 4.1a and 4.1b, and they are the same as in eq. 3.3 of the previous section.

4.3.2.2 v-symmetries

We will use the proposition of Paragraph 4.2 and a procedure analogous to the one of the above Section 4.3.2.1 in order to identify the v-classes at the present level $\lambda = 2$. Again, we will start separately for each of the two "old" sets $s_1^1(v)$ and $s_2^1(v)$.

1) Using the first "old" set $s_1^1(v)$:

From eq. 4.30, the "old" set contains only the class $S_{1,1}^1(v)$ (second column of Table 4.2a) which links the two nodes Pa and Pc. Therefore, $x_{1,1}^1$ = Pa and $x_{1,1}^2$ = Pc (third column of Table 4.2a). The two "new" sets of the present level $\lambda = 2$ are denoted as $s_1^2(v)$ and $s_2^2(v)$ and each contains two classes which - from the proposition eqs. 4.11

Table 4.2a: v-symmetry Classes at $\lambda = 2$. [Starting with $s_1^1(v)$]

Previous level (λ=1)				Present level (λ=2)	
m	Classes of "old" set	Node pairs	Variables w and w'	Classes of the first "new" set $s_1^2(v)$: $S_{1,j}^2(v)$={wa,w'c}	Classes of the second "new" set $s_2^2(v)$ $S_{2,j}^2(v)$={wb,w'd}
1	$S_{1,1}^4(v)$	$x_{1,1}^1$=Pa	w=$x_{1,1}^1$, w'=$x_{1,1}^2$	$S_{1,1}^2(v)$={Paa,Pcc}	$S_{2,1}^2(v)$={Pab,Pcd}
		$x_{1,1}^2$=Pc	w=$x_{1,1}^2$, w'=$x_{1,1}^1$	$S_{1,2}^2(v)$={Pca,Pac}	$S_{2,2}^2(v)$={Pcb,Pad}

and 4.13 - have the general forms:

$$S_{1,j}^2(v) = \{wa,\ w'c\}, \qquad j=1,2$$

and (4.36)

$$S_{2,j}^2(v) = \{wb,\ w'd\}, \qquad j=1,2$$

The resulting "new" classes at the present level $\lambda = 2$ are given in the fifth and sixth columns of Table 4.2a.

2) Using the second "old" set $s_2^1(v)$:

From eq. 4.31 the "old" set contains the class $S_{2,1}^1(v)$ (second column of Table 4.2b) which links the two nodes Pb and Pd. Therefore, $x_{2,1}^1 = Pb$ and $x_{2,1}^2 = Pd$ (third column of Table 4.2b). The two "new" sets of the present

Table 4.2b: v-symmetry Classes at $\lambda = 2$. [Starting with $s_2^1(v)$]

Previous level (λ=1)				Present level (λ=2)	
m	Classes of "old" set	Node pairs	Variables w and w'	Classes of the first "new" set $s_3^2(v)$: $S_{3,j}^2(v)=\{wa,w'c\}$	Classes of the second "new" set $s_4^2(v)$: $S_{4,j}^2(v)=\{wb,w'd\}$
1	$S_{2,1}^1(v)$	$x_{2,1}^1=Pb$	$w=x_{2,1}^1$, $w'=x_{2,1}^2$	$S_{3,1}^2(v)=\{Pba,Pdc\}$	$S_{4,1}^2(v)=\{Pbb,Pdd\}$
		$x_{2,1}^2=Pd$	$w=x_{2,1}^2$, $w'=x_{2,1}^1$	$S_{3,2}^2(v)=\{Pda,Pbc\}$	$S_{4,2}^2(v)=\{Pdb,Pbd\}$

level 2 are denoted as $s_3^2(v)$ and $s_4^2(v)$, and each contains two classes whose general forms are as in eq. 4.36 above. These classes are listed in the fifth and sixth columns of Table 4.2b.

Thus, for the v-symmetries at level 2, we have the following four sets of classes:

$$s_1^2(v) = \left\{S_{1,1}^2(v),\ S_{1,2}^2(v)\right\}$$

$$s_2^2(v) = \left\{S_{2,1}^2(v),\ S_{2,2}^2(v)\right\}$$

$$s_3^2(v) = \left\{ s_{3,1}^2(v),\ s_{3,2}^2(v) \right\}$$

$$s_4^2(v) = \left\{ s_{4,1}^2(v),\ s_{4,2}^2(v) \right\} \qquad (4.37)$$

Equation 4.37 is the same as eq. 3.11. The classes in eq. 4.37 are as defined in Tables 4.2a and 4.2b, and they are the same as in eq. 3.10.

4.3.2.3 r-symmetries

From eq. 4.32 there is only one "old" set at the previous level $\lambda = 1$, containing only one class $S_{1,1}^1(r)$ (second column of Table 4.3) linking the two nodes Pb and Pc. From the proposition of Paragraph 4.2, we see that, at this new higher level of refinement $\lambda = 2$, there

Table 4.3: r-symmetry Classes at $\lambda = 2$.

Previous level (λ=1)				Present level (λ=2)		
m	Classes of "old" set	Node pairs	Variables w and w'	Classes of the first "new" set $s_1^2(r)$: $S_{1,j}^2(r)$={wb,w'c}	Classes of the second "new" set $s_2^2(r)$: $S_{2,j}^2(r)$={wa,w'a}	Classes of the third "new" set $s_3^2(r)$: $S_{3,j}^2(r)$={wd,w'd}
1	$S_{1,1}^1(r)$	$x_{1,1}^1$=Pb	$w=x_{1,1}^1, w'=x_{1,1}^2$	$S_{1,1}^2(r)$={Pbb,Pcc}	$S_{2,1}^2(r)$={Pba,Pca}	$S_{3,1}^2(r)$={Pbd,Pcd}
		$x_{1,1}^2$=Pc	$w=x_{1,1}^2, w'=x_{1,1}^1$	$S_{1,2}^2(r)$={Pcb,Pbc}		

are at most three "new" sets $s_1^2(r)$, $s_2^2(r)$, and $s_3^2(r)$. The number of classes that each new set contains was derived in Paragraph 3.4.4. In this case, the first new set contains two classes, while the other two new sets each contains only one class. From eqs. 4.15, 4.17 and

4.19, the classes of the respective three new sets have the following forms:

$$S^2_{1,j}(r) = \{wb,\ w'c\}\ ,\quad j=1,2$$
$$S^2_{2,j}(r) = \{wa,\ w'a\}\ ,\quad j=1 \qquad (4.38)$$
$$\text{and}\quad S^2_{3,j}(r) = \{wd,\ w'd\}\ ,\quad j=1$$

The resulting "new" classes at the present level $\lambda = 2$ are given in the fifth, sixth and seventh columns of Table 4.3.

Thus, for the r-symmetries at level 2, we have the following three sets of classes:

$$s^2_1(r) = \{S^2_{1,1}(r),\ S^2_{1,2}(r)\}$$
$$s^2_2(r) = \{S^2_{2,1}(r)\} \qquad (4.39)$$
$$s^2_3(r) = \{S^2_{3,1}(r)\}$$

Equation 4.39 is the same as eq. 3.18. The classes in eq. 4.39 are listed in Table 4.3 and they are the same as in eq. 3.17.

4.3.2.4 ℓ-symmetries

From eq. 4.33 there is only one "old" set containing the class $S^1_{1,1}(\ell)$(second column of Table 4.4) which links the two nodes Pa and Pd. From the proposition we see that, at this new higher level of refinement $\lambda = 2$, there are again at most three "new" sets, denoted as $s^2_1(\ell)$, $s^2_2(\ell)$, and $s^2_3(\ell)$. The number of classes that each new set contains was derived in paragraph 3.5.4. Again, the first new set contains two classes, while the other two new sets each contain only one class. From eqs. 4.21, 4.23, and 4.25 the classes of the respective

three new sets have the following forms:

$$S^2_{1,j}(\ell) = \{wa,\ w'd\},\quad j=1,2$$

$$S^2_{2,j}(\ell) = \{wb,\ w'b\},\quad j=1 \qquad (4.40)$$

and $$S^2_{3,j}(\ell) = \{wc,\ w'c\},\quad j=1$$

The resulting "new" classes at the present level $\lambda = 2$ are given in the fifth, sixth, and seventh columns of Table 4.4.

Table 4.4: ℓ-symmetry classes at $\lambda = 2$

Previous level (λ=1)				Present level (λ=2)		
m	Classes of "old" set	Node pairs	Variables w and w'	Classes of the first "new" set $s^2_1(\ell)$: $S^2_{1,j}(\ell)$={wa,w'd}	Classes of the second "new" set $s^2_2(\ell)$: $S^2_{2,j}(\ell)$={wb,w'b}	Classes of the third "new" set $s^2_3(\ell)$: $S^2_{3,j}(\ell)$={wc,w'c}
1	$S^1_{1,1}(\ell)$	$x^1_{1,1}$=Pa	$w=x^1_{1,1}, w'=x^2_{1,1}$	$S^2_{1,1}(\ell)$={Paa,Pdd}	$S^2_{2,1}(\ell)$={Pab,Pdb}	$S^2_{3,1}(\ell)$={Pac,Pdc}
		$x^2_{1,1}$=Pd	$w=x^2_{1,1}, w'=x^1_{1,1}$	$S^2_{1,2}(\ell)$={Pda,Pad}		

Thus, for the ℓ-symmetries at level 2, we have the following three sets of classes:

$$s^2_1(\ell) = \{S^2_{1,1}(\ell),\ S^2_{1,2}(\ell)\}$$

$$s^2_2(\ell) = \{S^2_{2,1}(\ell)\} \qquad (4.41)$$

$$s^2_3(\ell) = \{S^2_{3,1}(\ell)\}$$

Equation 4.41 is the same as eq. 3.24. The classes in eq. 4.41 are listed in Table 4.4 and they are the same as in eq. 3.23.

4.3.3 Level 3 (i.e. $\lambda = 3$)

4.3.3.1 h-symmetries

From eq. 4.35 we see that at the previous level $\lambda = 2$ there were four different sets $s_1^2(h)$, $s_2^2(h)$, $s_3^2(h)$, and $s_4^2(h)$. Therefore, our procedure here is subdivided into four parts, each part starting with the classes of one of the above four sets. Again, at this new level of refinement, we have for each "old" set at most two "new" sets, each containing $t=2^{3-1} = 4$ classes. Our procedure for identifying the classes at level 3 is as follows:

1) Using the first "old" set $s_1^2(h)$:

From eq. 4.35 the "old" set contains two classes $S_{1,1}^2(h)$ and $S_{1,2}^2(h)$, as shown in the second column of Table 4.5a. The first class links the two nodes Paa and Pbb, while the second links the two nodes Pba and Pab. Therefore, $x_{1,1}^1$ = Paa , $x_{1,1}^2$ = Pbb , $x_{1,2}^1$ = Pba and $x_{1,2}^2$ = Pab, as listed in the third column of Table 4.5a. The fourth column of Table 4.5a lists the values of the variables w and w' as they are defined in eq. 4.3.

At the present level of refinement $\lambda = 3$, there are at most two "new" sets--denoted as $s_1^3(h)$ and $s_2^3(h)$--each containing four classes which, from the proposition eqs. 4.7 and 4.8, have the general forms:

$$\begin{aligned} &\text{the classes of the } s_1^3(h): \quad S_{1,j}^3(h) = \{wa,\ w'b\},\ j=1,2,3,4 \\ &\text{the classes of the } s_2^3(h): \quad S_{2,j}^3(h) = \{wc,\ w'd\},\ j=1,2,3,4 \end{aligned} \tag{4.42}$$

Table 4.5a: h-symmetry classes at $\lambda = 3$. [Starting with $s_1^2(h)$]

Previous level (λ=2)				Present level (λ=3)	
m	Classes of "old" set	Node pairs	Variables w and w'	Classes of the first "new" set $s_1^3(h)$: $S_{1,j}^3(h)$={wa,w'b}	Classes of the second "new" set $s_2^3(h)$: $S_{2,j}^3(h)$={wc,w'd}
1	$S_{1,1}^2(h)$	$x_{1,1}^1$=Paa	w=$x_{1,1}^1$, w'=$x_{1,1}^2$	$S_{1,1}^3(h)$={Paaa,Pbbb}	$S_{2,1}^3(h)$={Paac,Pbbd}
		$x_{1,1}^2$=Pbb	w=$x_{1,1}^2$, w'=$x_{1,1}^1$	$S_{1,2}^3(h)$={Pbba,Paab}	$S_{2,2}^3(h)$={Pbbc,Paad}
2	$S_{1,2}^2(h)$	$x_{1,2}^1$=Pba	w=$x_{1,2}^1$, w'=$x_{1,2}^2$	$S_{1,3}^3(h)$={Pbaa,Pabb}	$S_{2,3}^3(h)$={Pbac,Pabd}
		$x_{1,2}^2$=Pab	w=$x_{1,2}^2$, w'=$x_{1,2}^1$	$S_{1,4}^3(h)$={Paba,Pbab}	$S_{2,4}^3(h)$={Pabc,Pbad}

where the values of w and w' are given in the fourth column of Table 4.5a. The resulting "new" classes at the present level $\lambda = 3$ are given in the fifth and sixth column of Table 4.5a. In this case, m takes on the values 1 and 2, as shown in the first column of the table.

2) Using the second "old" set $s_2^2(h)$:

Again, from eq. 4.35 the "old" set contains two classes $S_{2,1}^2(h)$ and $S_{2,2}^2(h)$, as shown in the second column of Table 4.5b. The first class links the two nodes Pac and Pbd, while the second links the two nodes Pbc and Pad. Therefore, $x_{2,1}^1$ = Pac, $x_{2,1}^2$ = Pbd, $x_{2,2}^1$ = Pbc, and $x_{2,2}^2$ = Pad, as listed in the third column of Table 4.5b.

Table 4.5b: h-symmetry classes at $\lambda = 3$. [Starting with $s_2^2(h)$].

Previous level (λ=2)				Present level (λ=3)	
m	Classes of "old" set	Node pairs	Variables w and w'	Classes of the first "new" set $s_3^3(h)$: $S_{3,j}^3(h)=\{wa,w'b\}$	Classes of the second "new" set $s_4^3(h)$: $S_{4,j}^3(h)=\{wc,w'd\}$
1	$S_{2,1}^2(h)$	$x_{2,1}^1$=Pac	$w=x_{2,1}^1$, $w'=x_{2,1}^2$	$S_{3,1}^3(h)=\{Paca,Pbdb\}$	$S_{4,1}^3(h)=\{Pacc,Pbdd\}$
		$x_{2,1}^2$=Pbd	$w=x_{2,1}^2$, $w'=x_{2,1}^1$	$S_{3,2}^3(h)=\{Pbda,Pacb\}$	$S_{4,2}^3(h)=\{Pbdc,Pacd\}$
2	$S_{2,2}^2(h)$	$x_{2,2}^1$=Pbc	$w=x_{2,2}^1$, $w'=x_{2,2}^2$	$S_{3,3}^3(h)=\{Pbca,Padb\}$	$S_{4,3}^3(h)=\{Pbcc,Padd\}$
		$x_{2,2}^2$=Pad	$w=x_{2,2}^2$, $w'=x_{2,2}^1$	$S_{3,4}^3(h)=\{Pada,Pbcb\}$	$S_{4,4}^3(h)=\{Padc,Pbcd\}$

The variables w and w' are defined from eq. 4.3 and have the values listed in the fourth column of the Table. The two "new" sets of the present level $\lambda = 3$ are denoted as $s_3^3(h)$ and $s_4^3(h)$, and each contains four classes whose general forms are as in eq. 4.42 above. These classes are shown in the fifth and sixth columns of Table 4.5b.

3) Using the third "old" set $s_3^2(h)$:

Again, the "old" set contains two classes $S_{3,1}^2(h)$ and $S_{3,2}^2(h)$ as shown in the second column of Table 4.5c. The first class links the two nodes Pca and Pdb, while the second links the two nodes Pda and Pcb. Therefore, $x_{3,1}^1$ = Pca , $x_{3,1}^2$ = Pdb , $x_{3,2}^1$ = Pda , and $x_{3,2}^2$ = Pcb, as listed in the third column of

Table 4.5c: h-symmetry classes at $\lambda = 3$. [Starting with $s_3^2(h)$]

Previous level (λ=2)				Present level (λ=3)	
m	Classes of "old" set	Node pairs	Variables w and w'	Classes of the first "new" set $s_5^3(h)$: $S_{5,j}^3(h)$={wa,w'b}	Classes of the second "new" set $s_6^3(h)$: $S_{6,j}^3(h)$={wc,w'd}
1	$S_{3,1}^2(h)$	$x_{3,1}^1$=Pca	$w=x_{3,1}^1$, $w'=x_{3,1}^2$	$S_{5,1}^3(h)$={Pcaa,Pdbb}	$S_{6,1}^3(h)$={Pcac,Pdbd}
		$x_{3,1}^2$=Pdb	$w=x_{3,1}^2$, $w'=x_{3,1}^1$	$S_{5,2}^3(h)$={Pdba,Pcab}	$S_{6,2}^3(h)$={Pdbc,Pcad}
2	$S_{3,2}^2(h)$	$x_{3,2}^1$=Pda	$w=x_{3,2}^1$, $w'=x_{3,2}^2$	$S_{5,3}^3(h)$={Pdaa,Pcbb}	$S_{6,3}^3(h)$={Pdac,Pcbd}
		$x_{3,2}^2$=Pcb	$w=x_{3,2}^2$, $w'=x_{3,2}^1$	$S_{5,4}^3(h)$={Pcba,Pdab}	$S_{6,4}^3(h)$={Pcbc,Pdad}

Table 4.5c. The variables w and w' are defined as in the fourth column of the Table. The two "new" sets of the present level $\lambda = 3$ are denoted as $s_5^3(h)$ and $s_6^3(h)$, and each contains four classes whose general forms are again as in eq. 4.42 above. These classes are shown in the fifth and sixth columns of Table 4.5c.

4) Using the fourth "old" set $s_4^2(h)$:

Again, the "old" set contains two classes $S_{4,1}^2(h)$ and $S_{4,2}^2(h)$ as shown in the second column of Table 4.5d. The first class links the two nodes Pcc and Pdd, while the second links the two nodes Pdc and Pcd. Therefore, $x_{4,1}^1$ = Pcc , $x_{4,1}^2$ = Pdd , $x_{4,2}^1$ = Pdc , and $x_{4,2}^2$ = Pcd, as listed in the third column of Table 4.5d. The

Table 4.5d: h-symmetry classes at $\lambda = 3$. [Starting with $s_4^2(h)$].

Previous level (λ=2)				Present level (λ=3)	
m	Classes of "old" set	Node pairs	Variables w and w'	Classes of the first "new" set $s_7^3(h)$: $S_{7,j}^3(h)=\{wa,w'b\}$	Classes of the second "new" set $s_8^3(h)$: $S_{8,j}^3(h)=\{wc,w'd\}$
1	$S_{4,1}^2(h)$	$x_{4,1}^1$=Pcc	$w=x_{4,1}^1$, $w'=x_{4,1}^2$	$S_{7,1}^3(h)=\{Pcca,Pddb\}$	$S_{8,1}^3(h)=\{Pccc,Pddd\}$
		$x_{4,1}^2$=Pdd	$w=x_{4,1}^2$, $w'=x_{4,1}^1$	$S_{7,2}^3(h)=\{Pdda,Pccb\}$	$S_{8,2}^3(h)=\{Pddc,Pccd\}$
2	$S_{4,2}^2(h)$	$x_{4,2}^1$=Pdc	$w=x_{4,2}^1$, $w'=x_{4,2}^2$	$S_{7,3}^3(h)=\{Pdca,Pcdb\}$	$S_{8,3}^3(h)=\{Pdcc,Pcdd\}$
		$x_{4,2}^2$=Pcd	$w=x_{4,2}^2$, $w'=x_{4,2}^1$	$S_{7,4}^3(h)=\{Pcda,Pdcb\}$	$S_{8,4}^3(h)=\{Pcdc,Pdcd\}$

variables w and w' are defined as in the fourth column of the Table. The two "new" sets of the present level $\lambda = 3$ are denoted as $s_7^3(h)$ and $s_8^3(h)$, and each contains four classes whose general forms are again as in eq. 4.42 above. These classes are shown in the fifth and sixth columns of Table 4.5d.

Thus, for the h-symmetries at level 3, we have the following eight sets of classes:

$$
\begin{aligned}
s_1^3(h) &= \{S_{1,1}^3(h),\ S_{1,2}^3(h),\ S_{1,3}^3(h),\ S_{1,4}^3(h)\}\\
s_2^3(h) &= \{S_{2,1}^3(h),\ S_{2,2}^3(h),\ S_{2,3}^3(h),\ S_{2,4}^3(h)\}\\
s_3^3(h) &= \{S_{3,1}^3(h),\ S_{3,2}^3(h),\ S_{3,3}^3(h),\ S_{3,4}^3(h)\}\\
s_4^3(h) &= \{S_{4,1}^3(h),\ S_{4,2}^3(h),\ S_{4,3}^3(h),\ S_{4,4}^3(h)\}\\
s_5^3(h) &= \{S_{5,1}^3(h),\ S_{5,2}^3(h),\ S_{5,3}^3(h),\ S_{5,4}^3(h)\}\\
s_6^3(h) &= \{S_{6,1}^3(h),\ S_{6,2}^3(h),\ S_{6,3}^3(h),\ S_{6,4}^3(h)\}\\
s_7^3(h) &= \{S_{7,1}^3(h),\ S_{7,2}^3(h),\ S_{7,3}^3(h),\ S_{7,4}^3(h)\}\\
s_8^3(h) &= \{S_{8,1}^3(h),\ S_{8,2}^3(h),\ S_{8,3}^3(h),\ S_{8,4}^3(h)\}
\end{aligned}
\qquad (4.43)
$$

Equation 4.43 is the same as eq. 3.6 of the previous Section 3. The classes in eq. 4.43 are as defined in Tables 4.5a, 4.5b, 4.5c, and 4.5d, and they are the same as in eq. 3.5.

4.3.3.2 v-symmetries

From eq. 4.37 we see that at the previous level $\lambda = 2$ there were four different sets $s_1^2(v)$, $s_2^2(v)$, $s_3^2(v)$, and $s_4^2(v)$. Therefore, again our procedure is subdivided into four parts, one part for the classes of each of the above four sets. For each "old" set we have at most two "new" sets, each containing $t = 2^{3-1} = 4$ classes. The procedure is as follows:

1) Using the first "old" set $s_1^2(v)$:

From eq. 4.37 the "old" set contains two classes $S_{1,1}^2(v)$ and $S_{1,2}^2(v)$ as shown in the second column of Table 4.6a.

The first class links the two nodes Paa and Pcc (Table 4.2a),

Table 4.6a: v-symmetry classes at $\lambda = 3$. [Starting with $s_1^2(v)$].

Previous level (λ=2)				Present level (λ=3)	
m	Classes of "old" set	Node pairs	Variables w and w'	Classes of the first "new" set $s_1^3(v)$: $S_{1,j}^3(v)$={wa,w'c}	Classes of the second "new" set $s_2^3(v)$ $S_{2,j}^3(v)$={wb,w'd}
1	$S_{1,1}^2(v)$	$x_{1,1}^1$=Paa	$w=x_{1,1}^1$, $w'=x_{1,1}^2$	$S_{1,1}^3(v)$={Paaa,Pccc}	$S_{2,1}^3(v)$={Paab,Pccd}
		$x_{1,1}^2$=Pcc	$w=x_{1,1}^2$, $w'=x_{1,1}^1$	$S_{1,2}^3(v)$={Pcca,Paac}	$S_{2,2}^3(v)$={Pccb,Paad}
2	$S_{1,2}^2(v)$	$x_{1,2}^1$=Pca	$w=x_{1,2}^1$, $w'=x_{1,2}^2$	$S_{1,3}^3(v)$={Pcaa,Pacc}	$S_{2,3}^3(v)$={Pcab,Pacd}
		$x_{1,2}^2$=Pac	$w=x_{1,2}^2$, $w'=x_{1,2}^1$	$S_{1,4}^3(v)$={Paca,Pcac}	$S_{2,4}^3(v)$={Pacb,Pcad}

while the second links the two nodes Pca and Pac. Therefore, $x^1_{1,1}$ = Paa , $x^2_{1,1}$ = Pcc , $x^1_{1,2}$ = Pca and $x^2_{1,2}$ = Pac, as listed in the third column of Table 4.6a. The fourth column of the table lists the values of the variables w and w' as they are defined in eq. 4.3. At the present level of refinement $\lambda = 3$, there are at most two "new" sets--denoted as $s^3_1(v)$ and $s^3_2(v)$ -- each containing four classes which, from the proposition eqs. 4.11 and 4.13, have the general forms:

$$\begin{aligned} &\text{the classes of the } s^3_1(v): \quad S^3_{1,j}(v) = \{wa, w'c\},\ j=1,2,3,4 \\ &\text{the classes of the } s^3_2(v): \quad S^3_{2,j}(v) = \{wb, w'd\},\ j=1,2,3,4 \end{aligned} \tag{4.44}$$

where the values of w and w' are given in the fourth column of Table 4.6a. The resulting "new" classes at the present level $\lambda = 3$ are given in the fifth and sixth column of Table 4.6a. Again, like in the h-symmetries, the w takes on the values 1 and 2.

2) Using the second "old" set $s^2_2(v)$:

Again from eq. 4.37 the "old" set contains two classes $S^2_{2,1}(v)$ and $S^2_{2,2}(v)$, as shown in the second column of Table 4.6b. The first class links the two nodes Pab and Pcd, while the second links the two nodes Pcb and Pad.

Table 4.6b: v-symmetry classes at $\lambda = 3$. [Starting with $s_2^2(v)$].

Previous level (λ=2)				Present level (λ=3)	
m	Classes of "old" set	Node pairs	Variables w and w'	Classes of the first "new" set $s_3^3(v)$: $S_{3,j}^3(v)$={wa,w'c}	Classes of the second "new" set $s_4^3(v)$: $S_{4,j}^3(v)$={wb,w'd}
1	$S_{2,1}^2(v)$	$x_{2,1}^1$=Pab	$w=x_{2,1}^1$, $w'=x_{2,1}^2$	$S_{3,1}^3(v)$={Paba,Pcdc}	$S_{4,1}^3(v)$={Pabb,Pcdd}
		$x_{2,1}^2$=Pcd	$w=x_{2,1}^2$, $w'=x_{2,1}^1$	$S_{3,2}^3(v)$={Pcda,Pabc}	$S_{4,2}^3(v)$={Pcdb,Pabd}
2	$S_{2,2}^2(v)$	$x_{2,2}^1$=Pcb	$w=x_{2,2}^1$, $w'=x_{2,2}^2$	$S_{3,3}^3(v)$={Pcba,Padc}	$S_{4,3}^3(v)$={Pcbb,Padd}
		$x_{2,2}^2$=Pad	$w=x_{2,2}^2$, $w'=x_{2,2}^1$	$S_{3,4}^3(v)$={Pada,Pcbc}	$S_{4,4}^3(v)$={Padb,Pcbd}

Therefore, $x_{2,1}^1$ = Pab, $x_{2,1}^2$ = Pcd, $x_{2,2}^1$ = Pcb, and $x_{2,2}^2$ = Pad, as listed in the third column of Table 4.6b. The variables w and w' are defined from eq. 4.3 and have the values listed in the fourth column of the table. The two "new" sets of the present level $\lambda = 3$ are denoted as $s_3^3(v)$ and $s_4^3(v)$, and each contains four classes whose general forms are as in eq. 4.44 above. These classes are shown in the fifth and sixth columns of Table 4.6b.

3) Using the third "old" set $s_3^2(v)$:

Again, the "old" set contains two classes $S_{3,1}^2(v)$ and $S_{3,2}^2(v)$ as shown in the second column of Table 4.6c. The first class links the two nodes Pba and Pdc, while the second links the two nodes Pda and Pbc (Table 4.2b). Therefore, $x_{3,1}^1$ = Pba, $x_{3,1}^2$ = Pdc, $x_{3,2}^1$ = Pda and $x_{3,2}^2$ = Pbc,

Table 4.6c: v-symmetry classes at $\lambda = 3$. [Starting with $s_3^2(v)$].

Previous level (λ=2)				Present level (λ=3)	
m	Classes of "old" set	Node pairs	Variables w and w'	Classes of the first "new" set $s_5^3(v)$: $S_{5,j}^3(v)$={wa,w'c}	Classes of the second "new" set $s_6^3(v)$: $S_{6,j}^3(v)$={wb,w'd}
1	$S_{3,1}^2(v)$	$x_{3,1}^1$=Pba	w=$x_{3,1}^1$, w'=$x_{3,1}^2$	$S_{5,1}^3(v)$={Pbaa,Pdcc}	$S_{6,1}^3(v)$={Pbab,Pdcd}
		$x_{3,1}^2$=Pdc	w=$x_{3,1}^2$, w'=$x_{3,1}^1$	$S_{5,2}^3(v)$={Pdca,Pbac}	$S_{6,2}^3(v)$={Pdcb,Pbad}
2	$S_{3,2}^2(v)$	$x_{3,2}^1$=Pda	w=$x_{3,2}^1$, w'=$x_{3,2}^2$	$S_{5,3}^3(v)$={Pdaa,Pbcc}	$S_{6,3}^3(v)$={Pdab,Pbcd}
		$x_{3,2}^2$=Pbc	w=$x_{3,2}^2$, w'=$x_{3,2}^1$	$S_{5,4}^3(v)$={Pbca,Pdac}	$S_{6,4}^3(v)$={Pbcb,Pdad}

as listed in the third column of Table 4.6c. The two "new" sets of the present level $\lambda = 3$ are denoted as $s_5^3(v)$ and $s_6^3(v)$, and each contains four classes whose general forms are again as in eq. 4.44 above. These classes are shown in the fifth and sixth columns of Table 4.6c.

4) Using the fourth "old" set $s_4^2(v)$:

Again, the "old" set contains two classes $S_{4,1}^2(v)$ and $S_{4,2}^2(v)$. The first class links the two nodes Pbb and Pdd, while the second links the two nodes Pdb and Pbd (Table 4.2b). Therefore, $x_{4,1}^1$ = Pbb, $x_{4,1}^2$ = Pdd, $x_{4,2}^1$ = Pdb, and $x_{4,2}^2$ = Pbd, as listed in the third column of Table 4.6d below. The two "new" sets of the present level $\lambda = 3$

Table 4.6d: v-symmetry classes at $\lambda = 3$. [Starting with $s_4^2(v)$].

Previous level (λ=2)				Present level (λ=3)	
m	Classes of "old" set	Node pairs	Variables w and w'	Classes of the first "new" set $s_7^3(v)$: $S_{7,j}^3(v)$={wa,w'c}	Classes of the second "new" set $s_8^3(v)$: $S_{8,j}^3(v)$={wb,w'd}
1	$S_{4,1}^2(v)$	$x_{4,1}^1$=Pbb	$w=x_{4,1}^1$, $w'=x_{4,1}^2$	$S_{7,1}^3(v)$={Pbba,Pddc}	$S_{8,1}^3(v)$={Pbbb,Pddd}
		$x_{4,1}^2$=Pdd	$w=x_{4,1}^2$, $w'=x_{4,1}^1$	$S_{7,2}^3(v)$={Pdda,Pbbc}	$S_{8,2}^3(v)$={Pddb,Pbbd}
2	$S_{4,2}^2(v)$	$x_{4,2}^1$=Pdb	$w=x_{4,2}^1$, $w'=x_{4,2}^2$	$S_{7,3}^3(v)$={Pdba,Pbdc}	$S_{8,3}^3(v)$={Pdbb,Pbdd}
		$x_{4,2}^2$=Pbd	$w=x_{4,2}^2$, $w'=x_{4,2}^1$	$S_{7,4}^3(v)$={Pbda,Pdbc}	$S_{8,4}^3(v)$={Pbdb,Pdbd}

are denoted as $s_7^3(v)$ and $s_8^3(v)$, and each contains four classes whose general forms are again as in eq. 4.44 above. These classes are shown in the fifth and sixth columns of Table 4.6d.

Thus, for the v-symmetries at level 3, we have the following eight sets of classes:

$$
\begin{aligned}
s_1^3(v) &= \{S_{1,1}^3(v),\ S_{1,2}^3(v),\ S_{1,3}^3(v),\ S_{1,4}^3(v)\} \\
s_2^3(v) &= \{S_{2,1}^3(v),\ S_{2,2}^3(v),\ S_{2,3}^3(v),\ S_{2,4}^3(v)\} \\
s_3^3(v) &= \{S_{3,1}^3(v),\ S_{3,2}^3(v),\ S_{3,3}^3(v),\ S_{3,4}^3(v)\} \\
s_4^3(v) &= \{S_{4,1}^3(v),\ S_{4,2}^3(v),\ S_{4,3}^3(v),\ S_{4,4}^3(v)\} \qquad (4.45) \\
s_5^3(v) &= \{S_{5,1}^3(v),\ S_{5,2}^3(v),\ S_{5,3}^3(v),\ S_{5,4}^3(v)\} \\
s_6^3(v) &= \{S_{6,1}^3(v),\ S_{6,2}^3(v),\ S_{6,3}^3(v),\ S_{6,4}^3(v)\} \\
s_7^3(v) &= \{S_{7,1}^3(v),\ S_{7,2}^3(v),\ S_{7,3}^3(v),\ S_{7,4}^3(v)\} \\
s_8^3(v) &= \{S_{8,1}^3(v),\ S_{8,2}^3(v),\ S_{8,3}^3(v),\ S_{8,4}^3(v)\}
\end{aligned}
$$

Equation 4.45 is the same as eq. 3.13 of the previous Section 3. The classes in eq. 4.45 are as defined in Tables 4.6a, 4.6b, 4.6c and 4.6d, and they are the same as in eq. 3.12.

4.3.3.3 r-symmetries

From eq. 4.39 we see that at the previous level $\lambda = 2$, there were three different sets $s_1^2(r)$, $s_2^2(r)$ and $s_3^2(r)$. Therefore, our procedure is now subdivided into three parts, one for the classes of each of the above three sets.

1) Using the first "old" set $s_1^2(r)$:

From eq. 4.39 the "old" set contains two classes $S_{1,1}^2(r)$ and $S_{1,2}^2(r)$ as shown in the second column of Table 4.7a. The first class links the two nodes Pbb and Pcc, while the second links the two nodes Pcb and Pbc (Table 4.3). Therefore, $x_{1,1}^1$ = Pbb, $x_{1,1}^2$ = Pcc, $x_{1,2}^1$ = Pcb and $x_{1,2}^2$ = Pbc, as listed in the third column of Table 4.7a. The fourth column of the table lists the values of the variable w and w'. At the present level of refinement $\lambda = 3$, there are at most three "new" sets, denoted as $s_1^3(r)$, $s_2^3(r)$ and $s_3^3(r)$. The number of classes that each new set contains was derived in paragraph 3.4.4. In this case, the first new set contains four classes, while the other two new sets each contain two classes. From eqs. 4.15, 4.17 and 4.19 of the proposition, the classes of the respective three new sets have the following forms:

Table 4.7a: r-symmetry classes at $\lambda = 3$. [Starting with $s_1^2(r)$].

Previous level (λ=2)				Present level (λ=3)		
m	Classes of "old" set	Node pairs	Variables w and w'	Classes of the first "new" set $s_1^3(r)$: $S^3_{1,j}(r)$={wb,w'c}	Classes of the second "new" set $s_2^3(r)$: $S^3_{2,j}(r)$={wa,w'a}	Classes of the third "new" set $s_3^3(r)$: $S^3_{3,j}(r)$={wd,w'd}
1	$S^2_{1,1}(r)$	$x^1_{1,1}$=Pbb	$w=x^1_{1,1}$, $w'=x^2_{1,1}$	$S^3_{1,1}(r)$={Pbbb,Pccc}	$S^3_{2,1}(r)$={Pbba,Pcca}	$S^3_{3,1}(r)$={Pbbd,Pccd}
		$x^2_{1,1}$=Pcc	$w=x^2_{1,1}$, $w'=x^1_{1,1}$	$S^3_{1,2}(r)$={Pccb,Pbbc}		
2	$S^2_{1,2}(r)$	$x^1_{1,2}$=Pcb	$w=x^1_{1,2}$, $w'=x^2_{1,2}$	$S^3_{1,3}(r)$={Pcbb,Pbcc}	$S^3_{2,2}(r)$={Pcba,Pbca}	$S^3_{3,2}(r)$={Pcbd,Pbcd}
		$x^2_{1,2}$=Pbc	$w=x^2_{1,2}$, $w'=x^1_{1,2}$	$S^3_{1,4}(r)$={Pbcb,Pcbc}		

the classes of the $s_1^3(r)$: $S^3_{1,j}(r) = \{wb,w'c\}$, j=1,2,3,4

the classes of the $s_2^3(r)$: $S^3_{2,j}(r) = \{wa,w'a\}$, j=1,2 (4.46)

the classes of the $s_3^3(r)$: $S^3_{3,j}(r) = \{wd,w'd\}$, j=1,2

The resulting "new" classes at the present level $\lambda = 3$, are given in the fifth, sixth and seventh columns of Table 4.7a.

2) Using the second "old" set $s_2^2(r)$:

From eq. 4.39 we see that at the previous level $\lambda = 2$, the "old" set contains only one class $S^2_{2,1}(r)$ which, from Table 4.3, links the two nodes Pba and Pca. Therefore, $x^1_{2,1}$ = Pba and $x^2_{2,1}$ = Pca, as shown in the third column of Table 4.7b. At this present level of refinement $\lambda = 3$,

Table 4.7b: r-symmetry classes at $\lambda = 3$. [Starting with $s_2^2(r)$].

Previous level (λ=2)				Present level (λ=3)		
m	Classes of "old" set	Node pairs	Variables w and w'	Classes of the first "new" set $s_4^3(r)$: $S^3_{4,j}(r)$={wb,w'c}	Classes of the second "new" set $s_5^3(r)$: $S^3_{5,j}(r)$={wa,w'a}	Classes of the third "new" set $s_6^3(r)$: $S^3_{6,j}(r)$={wd,w'd}
1	$S^2_{2,1}(r)$	$x^1_{2,1}$=Pba	$w=x^1_{2,1}$, $w'=x^2_{2,1}$	$S^3_{4,1}(r)$={Pbab,Pcac}	$S^3_{5,1}(r)$={Pbaa,Pcaa}	$S^3_{6,1}(r)$={Pbad,Pcad}
		$x^2_{2,1}$=Pca	$w=x^2_{2,1}$, $w'=x^1_{2,1}$	$S^3_{4,2}(r)$={Pcab,Pbac}		

there are at most three "new" sets, denoted as $s_4^3(r)$, $s_5^3(r)$, and $s_6^3(r)$. The first new set contains two classes, while the other two new sets each contain only one class, whose general forms are as in eq. 4.46 above. These classes are listed in the fifth, sixth and seventh columns of Table 4.7b.

3) Using the third "old" set $s_3^2(r)$:

From eq. 4.39, the "old" set contains only one class $S^2_{3,1}(r)$ which, from Table 4.3, links the two nodes Pbd and Pcd. Therefore, $x^1_{3,1}$ = Pbd and $x^2_{3,1}$ = Pcd as shown in the third column of Table 4.7c. At the present level of refinement $\lambda = 3$, there are again at most three "new" sets, denoted as $s_7^3(r)$, $s_8^3(r)$ and $s_9^3(r)$. The first new set contains two classes, while the other two each contain only one class, whose general

Table 4.7c: r-symmetry classes at $\lambda = 3$. [Starting with $s_3^2(r)$]

Previous level (λ=2)				Present level (λ=3)		
m	Classes of "old" set	Node pairs	Variables w and w'	Classes of the first "new" set $s_7^3(r)$: $S_{7,j}^3(r)$={wb,w'c}	Classes of the second "new" set $s_8^3(r)$: $S_{8,j}^3(r)$={wa,w'a}	Classes of third "new" set $s_9^3(r)$: $S_{9,j}^3(r)$={wd,w'd}
1	$S_{3,1}^2(r)$	$x_{3,1}^1$=Pbd	$w=x_{3,1}^1$, $w'=x_{3,1}^2$	$S_{7,1}^3(r)$={Pbdb,Pcdc}	$S_{8,1}^3(r)$={Pbda,Pcda}	$S_{9,1}^3(r)$={Pbdd,Pcdd}
		$x_{3,1}^2$=Pcd	$w=x_{3,1}^2$, $w'=x_{3,1}^1$	$S_{7,2}^3(r)$={Pcdb,Pbdc}		

forms are as in eq. 4.46 above. These classes are listed in the fifth, sixth and seventh columns of Table 4.7c.

Thus, for the r-symmetries at level 3, we have the following nine sets of classes:

$$
\begin{aligned}
s_1^3(r) &= \{S_{1,1}^3(r),\ S_{1,2}^3(r),\ S_{1,3}^3(r),\ S_{1,4}^3(r)\} \\
s_2^3(r) &= \{S_{2,1}^3(r),\ S_{2,2}^3(r)\} \\
s_3^3(r) &= \{S_{3,1}^3(r),\ S_{3,2}^3(r)\} \\
s_4^3(r) &= \{S_{4,1}^3(r),\ S_{4,2}^3(r)\} \\
s_5^3(r) &= \{S_{5,1}^3(r)\} \\
s_6^3(r) &= \{S_{6,1}^3(r)\} \\
s_7^3(r) &= \{S_{7,1}^3\ ,\ S_{7,2}^3\} \\
s_8^3(r) &= \{S_{8,1}^3(r)\} \\
s_9^3(r) &= \{S_{9,1}^3(r)\}
\end{aligned}
\qquad (4.47)
$$

Equation 4.47 is the same as eq. 3.20 of the previous Section 3. The classes in eq. 4.47 are as defined in Tables 4.7a, 4.7b and 4.7c, and they are the same as in eq. 3.19.

4.3.3.4 ℓ-symmetries

From eq. 4.41 we see that at the previous level $\lambda = 2$, there were three different sets $s_1^2(\ell)$, $s_2^2(\ell)$ and $s_3^2(\ell)$. Therefore, our procedure is again subdivided into three parts, one for the classes of each of the above three sets.

1) Using the first "old" set $s_1^2(\ell)$:

From eq. 4.41 the "old" set contains two classes $S_{1,1}^2(\ell)$ and $S_{1,2}^2(\ell)$ as shown in the second column of Table 4.8a. The first class links the two nodes Paa and Pdd, while the second links the two nodes Pda and Pad (Table 4.4). Therefore, $x_{1,1}^1$ = Paa, $x_{1,1}^2$ = Pdd, $x_{1,2}^1$ = Pda and $x_{1,2}^2$ = Pad, as listed in the third column of Table 4.8a. At the present level of refinement $\lambda = 3$, there are at most three "new" sets, denoted as $s_1^3(\ell)$, $s_2^3(\ell)$ and $s_3^3(\ell)$. The number of classes that each new set contains was derived in paragraph 3.5.4. In this case, the first new set contains four classes, while the other two new sets, each contain two classes. From eqs. 4.21, 4.23 and 4.25 of the proposition, the classes of the respective three new sets have the following forms:

Table 4.8a: ℓ-symmetry classes at $\lambda = 3$. [Starting with $s_1^2(\ell)$].

Previous level (λ=2)				Present level (λ=3)		
m	Classes of "old" set	Node pairs	Variables w and w'	Classes of the first "new" set $s_1^3(\ell)$: $S_{1,j}^3(\ell)$={wa,w'd}	Classes of the second "new" set $s_2^3(\ell)$: $S_{2,j}^3(\ell)$={wb,w'b}	Classes of the third "new" set $s_3^3(\ell)$: $S_{3,j}^3(\ell)$={wc,w'c}
1	$S_{1,1}^2(\ell)$	$x_{1,1}^1$=Paa	$w=x_{1,1}^1$, $w'=x_{1,1}^2$	$S_{1,1}^3(\ell)$={Paaa,Pddd}	$S_{2,1}^3(\ell)$={Paab,Pddb}	$S_{3,1}^3(\ell)$={Paac,Pddc}
		$x_{1,1}^2$=Pdd	$w=x_{1,1}^2$, $w'=x_{1,1}^1$	$S_{1,2}^3(\ell)$={Pdda,Paad}		
2	$S_{1,2}^2(\ell)$	$x_{1,2}^1$=Pda	$w=x_{1,2}^1$, $w'=x_{1,2}^2$	$S_{1,3}^3(\ell)$={Pdaa,Padd}	$S_{2,2}^3(\ell)$={Pdab,Padb}	$S_{3,2}^3(\ell)$={Pdac,Padc}
		$x_{1,2}^2$=Pad	$w=x_{1,2}^2$, $w'=x_{1,2}^1$	$S_{1,4}^3(\ell)$={Pada,Pdad}		

the classes of the $s_1^3(\ell)$: $S_{1,j}^3(\ell) = \{wa, w'd\}$, j=1,2,3,4

the classes of the $s_2^3(\ell)$: $S_{2,j}^3(\ell) = \{wb, w'b\}$, j=1,2 (4.48)

the classes of the $s_3^3(\ell)$: $S_{3,j}^3(\ell) = \{wc, w'c\}$, j=1,2

The resulting "new" classes at the present level $\lambda = 3$, are listed in the fifth, sixth, and seventh columns of Table 4.8a.

2) Using the second "old" set $s_2^2(\ell)$:

From eq. 4.41 we see that the "old" set contains only one class $S_{2,1}^2(\ell)$ which, from Table 4.4, links the two nodes Pab and Pdb. Therefore, $x_{2,1}^1$ = Pab and $x_{2,1}^2$ = Pdb, as shown in the third column of Table 4.8b. At this present

Table 4.8b: ℓ-symmetry classes at $\lambda = 3$. [Starting with $s_2^2(\ell)$].

Previous level (λ=2)				Present level (λ=3)		
m	Classes of "old" set	Node pairs	Variables w and w'	Classes of the first "new" set $s_4^3(\ell)$: $s_{4,j}^3(\ell)$={wa,w'd}	Classes of the second "new" set $s_5^3(\ell)$: $s_{5,j}^3(\ell)$={wb,w'b}	Classes of the third "new" set $s_6^3(\ell)$: $s_{6,j}^3(\ell)$={wc,w'c}
1	$s_{2,1}^2(\ell)$	$x_{2,1}^1$=Pab	w=$x_{2,1}^1$, w'=$x_{2,1}^2$	$s_{4,1}^3(\ell)$={Paba,Pdbd}	$s_{5,1}^3(\ell)$={Pabb,Pdbb}	$s_{6,1}^3(\ell)$={Pabc,Pdbc}
		$x_{2,1}^2$=Pdb	w=$x_{2,1}^2$, w'=$x_{2,1}^1$	$s_{4,2}^3(\ell)$={Pdba,Pabd}		

level of refinement $\lambda = 3$, there are at most three "new" sets, denoted as $s_4^3(\ell)$, $s_5^3(\ell)$ and $s_6^3(\ell)$. The first new set contains two classes, while the other two new sets each contain only one class, whose general forms are as in eq. 4.48 above. These classes are listed in the fifth, sixth, and seventh columns of Table 4.8b.

3) Using the third "old" set $s_3^2(\ell)$:

From eq. 4.41, the "old" set contains only one class $s_{3,1}^2(\ell)$ which, from Table 4.4, links the two nodes Pac and Pdc. Therefore, $x_{3,1}^1$ = Pac and $x_{3,1}^2$ = Pdc as shown in the third column of Table 4.8c. At the present level $\lambda = 3$, there are again at most three "new" sets, denoted as $s_7^3(\ell)$, $s_8^3(\ell)$ and $s_9^3(\ell)$. The first new set contains two classes and, each of the other two, one class, whose general forms are as in eq. 4.46 above. These classes are listed in the fifth, sixth and seventh columns of Table 4.8c.

Table 4.8c: ℓ-symmetry classes at $\lambda = 3$. [Starting with $s^2_3(\ell)$].

Previous level (λ=2)				Present level (λ=3)		
m	Classes of "old" set	Node pairs	Variables w and w'	Classes of the first "new" set $s^3_7(\ell)$: $S^3_{7,j}(\ell)$={wa,w'd}	Classes of the second "new" set $s^3_8(\ell)$: $S^3_{8,j}(\ell)$={wb,w'b}	Classes of the third "new" set $s^3_9(\ell)$: $S^3_{9,j}(\ell)$={wc,w'c}
1	$S^2_{3,1}(\ell)$	$x^1_{3,1}$=Pac	$w=x^1_{3,1}$, $w'=x^2_{3,1}$	$S^3_{7,1}(\ell)$={Paca,Pdcd}	$S^3_{8,1}(\ell)$={Pacb,Pdcb}	$S^3_{9,1}(\ell)$={Pacc,Pdcc}
		$x^2_{3,1}$=Pdc	$w=x^2_{3,1}$, $w'=x^1_{3,1}$	$S^3_{7,2}(\ell)$={Pdca,Pacd}		

Thus, for the ℓ-symmetries at level $\lambda = 3$, we have the following nine sets of classes:

$$
\begin{aligned}
s^3_1(\ell) &= \{S^3_{1,1}(\ell),\ S^3_{1,2}(\ell),\ S^3_{1,3}(\ell),\ S^3_{1,4}(\ell)\} \\
s^3_2(\ell) &= \{S^3_{2,1}(\ell),\ S^3_{2,2}(\ell)\} \\
s^3_3(\ell) &= \{S^3_{3,1}(\ell),\ S^3_{3,2}(\ell)\} \\
s^3_4(\ell) &= \{S^3_{4,1}(\ell),\ S^3_{4,2}(\ell)\} \\
s^3_5(\ell) &= \{S^3_{5,1}(\ell)\} \\
s^3_6(\ell) &= \{S^3_{6,1}(\ell)\} \\
s^3_7(\ell) &= \{S^3_{7,1}(\ell),\ S^3_{7,2}(\ell)\} \\
s^3_8(\ell) &= \{S^3_{8,1}(\ell)\} \\
s^3_9(\ell) &= \{S^3_{9,1}(\ell)\}
\end{aligned}
\qquad (4.49)
$$

Equation 4.49 is the same as eq. 3.26 of the previous Section 3. The classes in eq. 4.49 are as defined in Tables 4.8a, 4.8b and 4.8c, and they are the same as in eq. 3.25.

SECTION 5

CONCLUSIONS AND FURTHER WORK

In this report we have treated the general problem of extracting structural information from an object in a scene.

The scene is first decomposed into regions (subgrids), through the application of the regular decomposition procedure described in Section 2. The outcome of this decomposition is a dimensionally reduced tree data-structure where only the "informative" sections of the picture have been retained. Each tree node represents information about a particular zone of the picture, whose (the zone's) size and position depend upon the level and the location of the node in the tree. We have identified the nodes of the tree data-structure that correspond to picture subgrids at various directions, and have given their interrelationships. Only four directions are treated in this report, i.e., horizontal, vertical, left-diagonal and right-diagonal (although this can easily be extended to include other directions, too), and we have proposed a recursive algorithm which specifies the tree nodes--i.e., picture subregions of various sizes--that must be paired (or compared) to identify (or extract) possible directional symmetries present in the picture. This proposition has been tested on various symmetry data-structures and the results--given in tabular form, at various tree levels, for each of the four directional symmetries--proved to be valid.

For extensions to this work we plan to cover many other directional symmetries, for example, directions at angles of 15° apart. Having done this, we will present a complete ALGOL-like description of the

algorithm and results obtained by applying it to various pictures of both artificial and real scenes. Included in these experimental runs we propose to: (1) perform the regular decomposition tree data-structure based not only on average subgrid intensity but also on directional symmetries; (2) incorporate statistical parameters to each tree node, thus combining (or comparing) them to identify symmetries based on statistical measurements; (3) perform tree-mapping, i.e., transform one tree data-structure to another, in which the relationships between directional-symmetries and tree-nodes will be explicitly shown.

Although the subgrid sizes and shapes are fixed in this report, we can readily extend the method to include variable (and adaptive) sizes and shapes in performing our data-structure generation.

Our process may also be part of an on-line system (or picture-language) where the complicated object to be "decomposed" (fragmented, atomized) is identified through an algorithm which operates with guidance. For example, the operator may point out the part of the image that he proposes to the machine. The algorithm then can do all the necessary decomposing and matching.

Our process may also be used for performing a nonuniform and adaptive scan of the picture. Thus, under digital control, scene symmetries may be located by using a reflection of the scan--a dual scan--about a "stepped" test symmetry-axis. The width of this dual scan may also be adaptively varying, according to the level of the desired resolution of the scanner.

Finally, we believe that such a hierarchical decision based problem subdivision may well be compactly handled by formal grammars.

This work may be extended as follows:

1. Improve the regular decomposition algorithm by finding criteria that subdivide a region not necessarily in four equal parts, but in a number of parts, of various sizes, and along "directions of importance". For example, it may be fruitful to partition the picture along a certain direction where a strong symmetry has been identified.
2. Perform a mapping from the "regular decomposition tree" to a "directional symmetry tree", i.e., a tree which explicitly reflects symmetries present in the picture.
3. Increase the number of directions along which symmetries are being examined, e.g., at angles of 15°, and get the "symmetry histograms" of real scenes or objects (i.e., "degree of symmetry" vs. "angle").
4. Investigate how are certain patterns directly recognizable from their tree structure.
5. Modify the algorithm to dynamically (or, maybe, interactively) vary subgrid dimensions and/or shape, so that effectively the procedure will be focusing on "interesting" areas of the picture.
6. We plan to investigate the subquadrants' spatial and topological relationships (e.g., ADJACENT, ABOVE, etc.) with regards to their position on the tree representation of the image.
7. Simulation of adaptive picture scanning to locate scene symmetries.

8. Investigate efficient data structures for image representation and processing, so that parts of the data structure can be paged to peripheral storage.

REFERENCES

[1] Polya, G., Induction and Analogy in Mathematics, Vol. 1, Princeton University Press, 1954.

[2] Klinger, A., "Patterns and Search Statistics," in Optimizing Methods in Statistics, J. S. Rustagi (ed.), Academic Press, N. Y., 1971, pp. 303-339.

[3] Klinger, A., "Data Structures and Pattern Recognition," Proceedings First International Joint Conference on Pattern Recognition, Washington, D. C., 1973.

[4] Warnock, J. E., "A Hidden Surface Algorithm for Computer Generated Halftone Pictures," Computer Science Department, University of Utah, TR 4-15, June 1969.

[5] Rosen, C. A. and N. J. Nilsson, "Application of Intelligent Automata to Reconnaissance," SRI Project 5953, December 1967.

[6] Eastman, C. M., "Representations for Space Planning," Comm. ACM, Vol. 13, No. 4, April 1970.

[7] Nillson, N., Problem Solving Methods in Artificial Intelligence, McGraw-Hill, 1971.

[8] Rosenfeld, A., Picture Processing by Computer, Academic Press, N. Y., 1969.

[9] Rosenfeld, A., "Progress in Picture Processing: 1969-1971," ACM Computing Surveys, Vol. 5, No. 2, June 1973.

[10] Duda, R. O. and P. E. Hart, Pattern Classification and Scene Analysis, J. Wiley, 1973.

[11] Klinger, A., A. Kochman, and N. Alexandridis, "Computer Analysis of Chromosome Patterns: Feature Encoding for Flexible Decision Making," IEEE Transactions on Computers, C-20, pp. 1014-1022, September 1971.

[12] Merrill, R. D., "Representation of Contours and Regions for Efficient Computer Search," Comm. ACM, 16, 2, pp. 69-82, February 1973.

[13] Roberts, L. G., "Machine Perception of Three Dimensional Solids," Optical and Electro-Optical Information Processing, Tippett (ed.), MIT Press, Cambridge, 1965.

[14] Guzman, A., "Computer Recognition of Three Dimensional Objects in a Visual Scene," Department of Electrical Engineering, MIT, MAC-TR-59, 1968.

AD-A033 289 CALIFORNIA UNIV LOS ANGELES DEPT OF COMPUTER SCIENCE F/G 14/5
PICTURE DECOMPOSITION, TREE DATA-STRUCTURES AND IDENTIFYING DIR--ETC(U)
SEP 76 N ALEXANDRIDIS, A KLINGER AF-AFOSR-2384-72
UNCLASSIFIED UCLA-ENG-7684 AFOSR-TR-76-1220 NL

2 OF 2
AD
A033289

END

DATE
FILMED
2-77


3328
1.0
1.1
1.25
1.4
1.6
2.8
2.5
3.2
2.2
3.6
4.0
2.0
1.8
MICROCOPY RESOLUTION TEST CHART
NATIONAL BUREAU OF STANDARDS - 1963 - A

[15] Falk, G., "Computer Interpretation of Imperfect Line Data as in a Three Dimensional Scene," Department of Computer Science, Stanford University, AIM 139, 1970.

[16] Feng, H. Y. F. and T. Pavlidis, "The Generation of Polygonal Outlines of Objects from Gray Level Pictures," Department of Electrical Engineering, Princeton University, TR-150, April 1974.

[17] Minsky, M. and S. Papert, Project MAC Progress Report IV, MIT Press, Cambridge, 1967.

[18] Brice, C. R. and C. L. Fennema, "Scene Analysis Using Regions," Artificial Intelligence Journal, Vol. 1, No. 3, 1970, pp. 205-226.

[19] Yakimovsky, Y., "Scene Analysis Using a Semantic Base for Region Growing," Department of Computer Science, Stanford University, AIM 209, 1973.

[20] Sutherland, I., "Computer Displays," (Scientific American, June 1970) in Computers and Computations, Edited by R. R. Fenichel and J. Weizenbaum, W. H. Freeman and Co., San Francisco, 1971, pp. 52-69.

[21] Eastman, C. M. and C. I. Yessios, "An Efficient Algorithm for Finding the Union, Intersection and Differences in Spatial Domains," Department of Computer Science, Carnegie-Mellon University, September 1972.

[22] Freeman, H., "On the Encoding of Arbitrary Geometric Configurations," IRE Transactions on Computers, EC-10, pp. 260-268, June 1961.

[23] Newman, W. M. and R. F. Sproul, Principles of Interactive Computer Graphics, McGraw-Hill, 1973.

[24] Barrow, H. G. and R. J. Popplestone, "Relational Descriptions in Picture Processing," Machine Intelligence 6 (eds. B. Meltzer and D. Michie), Edingburgh: University Press, pp. 377-396, 1971.

[25] Barrow, H. G. and Milner, D., "A Hierarchical Picture Interpretation System with Directed Search," MIP-R-85, Department of Machine Intelligence and Perception, University of Edinburgh, 1971.

[26] Barrow, H. G., Ambler, A. P., and R. M. Burstall, "Some Techniques for Recognizing Structures in Pictures" in Frontiers of Pattern Recognition, (ed. by S. Watanabe), Academic Press, 1972.

[27] Pavlidis, T., "Representation of Figures by Labeled Graphs," Pattern Recognition, 4, pp. 6-18, 1972.

[28] Swain, P. H. and K. S. Fu, "Stochastic Programmed Grammars for Syntactic Pattern Recognition," Pattern Recognition, 4, pp. 83-100, 1972.

[29] Narasimhan, R. and V.S.N. Reddy, "A Syntax-aided Recognition Scene for Handprinted English Letters," Pattern Recognition, 3, pp. 345-362, 1971.

[30] Clowes, M., "Transformational Grammars and the Organization of Pictures," Automatic Interpretation and Classification of Images, A. Grasselli, ed., pp. 43-78, Academic Press, New York, 1969.

[31] Clowes, M., "On Seeing Things," Artificial Intelligence, 2, pp. 79-116, 1971.

[32] Miller, W. F. and A. C. Shaw, "Linguistic Methods in Picture Processing: A Survey," AFIPS, FJCC 33, Part 1, pp. 279-290, 1968.

[33] Fu, K. S., Syntactic Methods in Pattern Recognition, Academic Press, New York, 1969.

[34] Baird, M. L. and M. D. Kelly, "A Paradigm for Semantic Picture Recognition," Pattern Recognition, 6, pp. 61-74, 1974.

[35] Klinger, A., "Sampling Images: Search Statistics and Computer Pattern Recognition," Proceedings Computer Science and Statistics: 8th Annual Symposium on the Interface, Health Science Computing Facility, UCLA, Los Angeles, California 90024, pp. 439-446, February 1975.

[36] Klinger, A. and C. R. Dyer, "Experiments on Picture Representation Using Regular Decomposition," UCLA-ENG 7494, School of Engineering and Applied Science, UCLA, Los Angeles, California, December 1974.

[37] Klinger, A., "Regular Decomposition and Picture Structure," Proceedings 1974 International Conference on Systems, Man, and Cybernetics.

[38] Klinger, A. and G. H. Keludjian, "A Proposal for On-line Feature Detection and Extraction," Proceedings 1972 Computer Image Processing and Recognition Symposium.

[39] Arcelli, C., L. Cordella, and S. Levialdi, "Parallel Processing for Image Analysis," New Concepts and Technologies in Parallel Information Processing, E. R. Caianiello (ed.), NATO Advanced Institutes Series E, Applied Sciences, No. 9, pp. 105-121, 1973.

[40] Rosenfeld, A., "Isotonic Grammars, Parallel Grammars, and Picture Grammars," Machine Intelligence, B. Meltzer and D. Michie (eds.), Vol. 6, American Elsevier Publishing Company, Inc., 1971.

[41] Firschein, O. and M. A. Fischler, "Describing and Abstracting Pictorial Structures," Pattern Recognition, Vol. 3, No. 4, November 1971.

[42] Firschein, O. and M. A. Fischler, "A Study in Descriptive Representation of Pictorial Data," Pattern Recognition, Vol. 4, No. 4, December 1972.

[43] Pavlidis, T., "Analysis of Set Patterns," Pattern Recognition, Vol. 1, November 1968.

[44] Pavlidis, T., "Structural Pattern Recognition: Primitives and Juxtaposition Relations," in Frontiers of Pattern Recognition, S. Watanabe (ed.), Academic Press, New York, 1972.

[45] Kelly, M. D., "Edge Detection in Pictures by Computer Using Planning," Machine Intelligence, B. Meltzer and D. Michie (eds.), Vol. 6, American Elsevier Publishing Company, Inc., 1971, pp. 397-409.

[46] Pfalz, S. L., Snively, J. W., and A. Rosenfeld, "Local and Global Picture Processing by Computer," in "Pictorial Pattern Recognition," Proceedings of Symposium on Automatic Photointerpretation, G. C. Cheng, R. S. Ledley, P. K. Pollock, A. Rosenfeld (eds.), Thompson Book Company, 1968, pp. 353-371.